

CHEMISTRY

A European Journal



Accepted Article

Title: Improving the Switching Capacity of Glyco-SAMs on Au(111)

Authors: Felix Tuczec, Thisbe Lindhorst, Ellen Fast, Alexander Schlimm, Irene Lautenschläger, Kai Uwe Clausen, Thomas Strunskus, and Carina Spormann

This manuscript has been accepted after peer review and appears as an Accepted Article online prior to editing, proofing, and formal publication of the final Version of Record (VoR). This work is currently citable by using the Digital Object Identifier (DOI) given below. The VoR will be published online in Early View as soon as possible and may be different to this Accepted Article as a result of editing. Readers should obtain the VoR from the journal website shown below when it is published to ensure accuracy of information. The authors are responsible for the content of this Accepted Article.

To be cited as: *Chem. Eur. J.* 10.1002/chem.201903644

Link to VoR: <http://dx.doi.org/10.1002/chem.201903644>

Supported by
ACES

WILEY-VCH

FULL PAPER

Improving the Switching Capacity of Glyco-SAMs on Au(111)

Ellen Fast^{[a]#}, Alexander Schlimm^{[b]#}, Irene Lautenschläger^[b], Kai Uwe Clausen^[b], Thomas Strunskus^[c], Carina Spormann^[a], Thisbe K. Lindhorst^{[a]*}, Felix Tuczek^{[b]*}

Abstract: Self-assembled monolayers (SAMs) decorated with photoisomerizable azobenzene glycosides are useful tools to investigate the effect of ligand orientation on carbohydrate recognition. However, photoswitching of SAMs between two specific states is characterized by a limited capacity. The goal of this study is the improvement of photoswitchable azobenzene glyco-SAMs. Different concepts, in particular self-dilution and rigid biaryl backbones, were investigated. The required SH-functionalized azobenzene glycoconjugates were synthesized following a modular approach, the respective glyco-SAMs were fabricated on Au(111) and their photoswitching properties extensively investigated with a powerful set of methods (IRRAS, XPS and NEXAFS). Indeed, the combination of tailor-made biaryl-azobenzene glycosides and suitable diluter molecules led to photoswitchable glyco-SAMs with a significantly enhanced and unprecedented switching capacity.

Introduction

Many biological processes such as cell signalling, cell recognition, or cell adhesion are mediated by molecular interactions occurring at the cell surface, which is covered by a layer of diverse glycoconjugates, called the glycocalyx.^[1] Therefore, the elucidation of the mechanisms, which underlie carbohydrate recognition, is a key to our understanding of cell surface biology. Carbohydrates are ligands of a class of proteins, called lectins,^[2] which apparently govern much of cell-cell interactions by specific carbohydrate-lectin interactions. For example, many *Enterobacteriaceae* such as *Escherichia coli* (*E. coli*) accomplish firm adhesion to the surface of their host cells by lectins, which are constituents of adhesive organelles

projecting from the bacterial surface, called fimbriae (or pili).^[3] Among the most important bacterial fimbriae are so-called type 1 fimbriae, which mediate adhesion to terminal α -D-mannopyranoside components of the glycocalyx through the type 1-fimbrial lectin FimH.^[4]

Many principles of the highly complex supramolecular interactions leading to cell adhesion are still not well understood. Therefore, model systems, in particular so-called glyco-SAMs (self-assembled monolayers),^[5] were used to mimic the glycocalyx and to allow the investigation and interrogation of carbohydrate-protein interactions on surfaces. As a first step into this direction, we prepared glyco-SAMs derived from molecules composed of an azobenzene moiety, an alkanethiol linker and a mannoside head group and investigated them by XPS (X-ray photoelectron spectroscopy), NEXAFS (near-edge X-ray absorption fine structure) and IRRAS (infrared reflection-absorption spectroscopy).^[6] Here, photoisomerization of the azobenzene N=N double bond between two isomeric states (*trans* and *cis*) allows the reversible reorientation of a sugar ligand, if the molecule is properly adsorbed on a surface. Indeed, when conjugated to an alkanethiol chain, azobenzene glycosides self-assemble to monolayers on gold (Au(111)). Utilizing the intensity change of the C(aryl)-O(mannoside) stretching band upon *cis/trans*-isomerization (*E/Z* isomerization), we were in fact able to monitor a reversible, photoinduced switching of the orientation of the head group. Nevertheless, the observed intensity change was small (about 4 %). More recently, we showed the importance of ligand orientation in carbohydrate-specific bacterial adhesion using a SAM of azobenzene glycosides containing OEG (oligoethylene) moieties.^[7] When we applied this system to bacterial adhesion, the adhesion of type 1-fimbriated *E. coli* was greatly reduced in the *cis*- in comparison to the *trans*-state. Remarkably, photoswitching of azobenzene glycoconjugates also alters bacterial adhesion on cell surfaces.^[8]

Regarding the actual performance of photoswitchable glyco-SAMs, it is important to note that the *trans*→*cis* isomerization of the azobenzene moiety is associated with a large spatial change and, therefore, the molecules on the surface require enough free volume to undergo the isomerization. This, however, is in direct conflict with the nature of most SAMs which consist of densely packed molecules.^[9] Correspondingly, in our first study employing glycoazobenzene alkanethiols without an OEG group, less bulky alkanethiols were needed as diluter molecules to achieve *trans*→*cis* isomerization of the glycoazobenzenes in SAMs (Figure 1, a).^[6] On the other hand, when we switched bacterial adhesion, the employed SAMs containing OEG moieties and no further diluter molecules were used for the fabrication of the photoswitchable SAMs.^[7] The exact influence of the OEG groups on the switching properties of the respective glyco-SAMs is unclear.

These authors contributed equally to this paper.

[a] Ellen Fast, Carina Spormann, Thisbe K. Lindhorst
Otto Diels Institute of Organic Chemistry
Christian-Albrechts-University Kiel
Otto-Hahn-Platz 4, 24118 Kiel
tklind@oc.uni-kiel.de

[b] Alexander Schlimm, Irene Lautenschläger, Kai Uwe Clausen, Felix Tuczek
Institute of Inorganic Chemistry
Christian-Albrechts-University Kiel
Max-Eyth Straße 2, 24118 Kiel
ftuczek@ac.uni-kiel.de

[c] Thomas Strunskus
Institute for Materials Science – Multicomponent Materials
Christian-Albrechts-University Kiel
Kaisertr. 2, 24143

Supporting information for this article is given via a link at the end of the document.

FULL PAPER

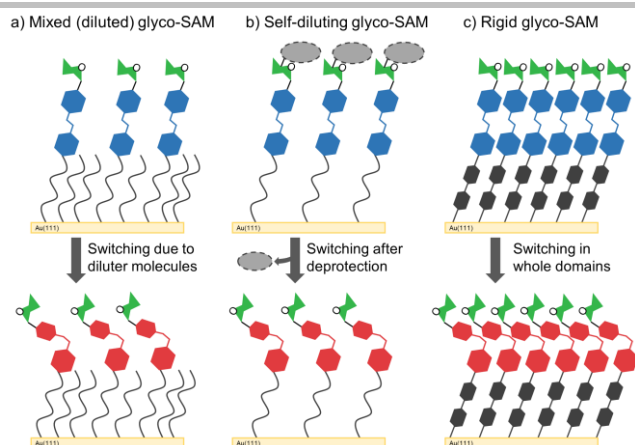


Figure 1. Three different approaches of photoswitchable glyco-SAMs, fabricated from azobenzene glycoconjugates: a) *Cis*→*trans* isomerization is facilitated by diluter molecules; b) concept of self-dilution; c) photoswitching of rigid (biphenyl-containing) SAMs. The *trans* (*E*)-state of the azobenzene hinge is shown in blue, the *cis* (*Z*)-state in red, the green sugar residue symbolizes α -D-mannopyranoside, and the grey oval a bulky protecting group.

In order to further improve the properties of photoswitchable glyco-SAMs, it is essential to understand the dependence of the switching capacity (i.e., the fraction of molecules undergoing photoinduced *cis/trans*-isomerization) on the physicochemical properties of the head groups and the underlying SAM. Key parameters in this regard are the rigidity of the chains contained in the molecules forming the SAM, their lateral density as well as their intermolecular interactions, and the free volume required for the switching of the head groups.^[10,11] A first approach to providing sufficient free volume for photoswitching was based on the application of non-planar substrates like nanoparticles. Because of the surface curvature of these particles, the adsorbed molecules have significantly more free volume than on a flat surface.^[10,12] Other concepts also allow effective photoisomerization on flat surfaces, such as the platform approach,^[13,14] where the size of a ring system which is adsorbed to a gold surface determines the intermolecular distances of the photoswitchable molecules mounted on this platform. This approach can be turned up-side down using bulky protecting groups, which provide space between the chemisorbed molecules during SAM formation and can be cleaved on the surface after the adsorption process. Lahann et al. showed that such SAMs are stable even after the deprotection step.^[15] This approach can be termed a self-diluting process (Figure 1, b). On the contrary, SAMs can also be fabricated from molecules based on rigid biphenyl backbones leading to especially densely packed monolayers due to strong intermolecular π - π interactions (Figure 1, c). Counterintuitively, such SAMs, consisting of azobenzene-biphenyl thiols for example, show excellent switching properties on surfaces.^[16] Pace et al. attributed these results to a cooperative character of the switching process.^[16]

Herein, we adapt both of these approaches towards effective photoisomerization of azobenzene-containing SAMs (i.e., Figure 1 b and c)^[15,16] to the design of new azobenzene glyco-SAMs, in order to investigate whether we find an improved switching behavior. Because of its biological importance, azobenzene α -D-

mannoside was selected as photoswitchable carbohydrate ligand, as in our earlier work.^[6,7] Regarding the self-diluting approach, the 6-position of the mannopyranoside ring forms an ideal attachment point for a bulky protecting group. For the fabrication of rigid SAMs, aryl-aryl cross coupling reactions were employed to conjugate azobenzene α -D-mannoside to a rigid backbone. The chemical composition and the integrity of the prepared SAMs were determined by XPS, and their switching capacities were investigated using a combination of IRRAS and NEXAFS.

Results and Discussion

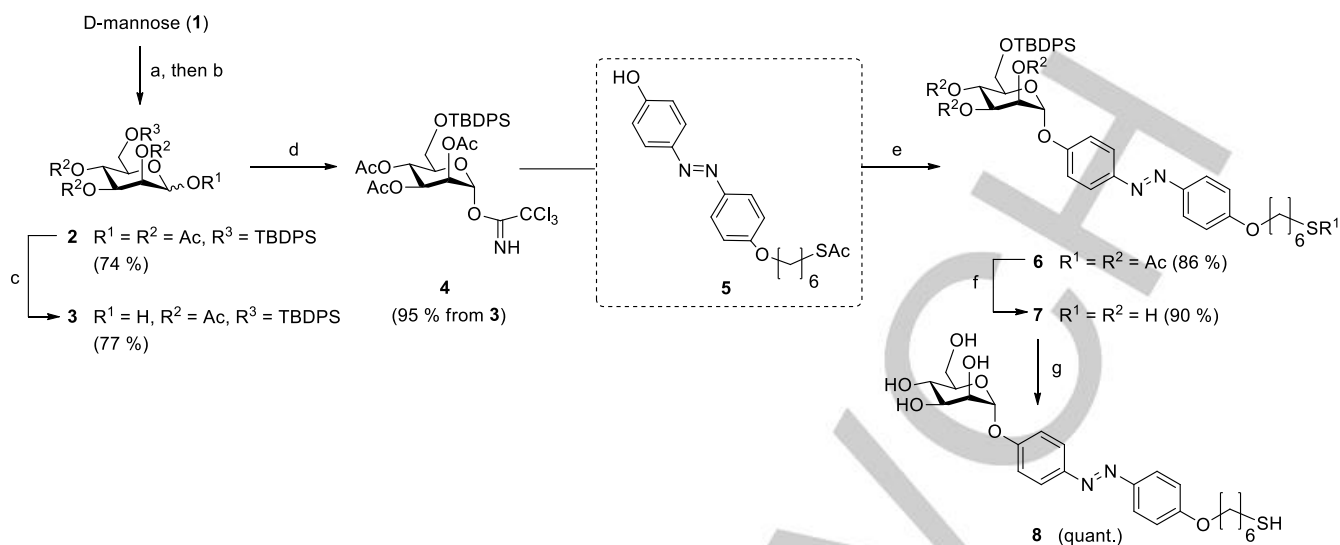
1. Synthesis

For the fabrication of self-diluting SAMs (cf. Figure 1, b) glycoazobenzene alkanethiols are required, carrying a bulky protecting group which can be cleaved under mild conditions on the SAM surface. The primary hydroxy group of the sugar moiety is a practical position for the installation of a bulky moiety as it is amenable to a regioselective reaction. In first attempts, a trityl group was selected for the modification of 6-OH, however, it caused problems in later steps of the synthesis. Then, a *tert*-butyldiphenylsilyl (TBDS) ether was chosen for the protection of the 6-position of the sugar, which can be cleaved under mild acidic conditions or by fluoride ions. This approach works very well even with free D-mannose, where the regioselective silylation of the 6-hydroxy group and a subsequent acetylation step, in order to protect the secondary OH-groups, furnished the mannose tetraacetate **2** in 74 % over 2 steps (Scheme 1). This derivative was then converted into a mannosyl donor, first by selective deprotection of the anomeric position employing ethylenediamine in a mixture with acetic acid^[17] and secondly by the base-promoted addition of the reducing sugar **3** to trichloroacetonitrile to yield the *O*-mannosyl trichloroacetimidate **4**,^[18] carrying the requested bulky protecting group at C-6.

In the following mannosylation step, the hydroxy azobenzene derivative **5** served as glycosyl acceptor. It carries the aliphatic 6-acetylthio-hexanyl linker, which is required for the fabrication of SAMs. It was obtained by selective nucleophilic substitution of 6-acetylthio-1-hexanesulfonate with dihydroxyazobenzene (cf. SI). The Lewis acid-promoted reaction of **4** with **5** under standard conditions^[19] gave the desired mannoside **6** in excellent yield and as sole α -anomer. Treatment of the protected mannoside **6** with sodium methanolate in methanol to liberate both the OH-groups and the thiol group gave **7** in 90 %. When this thiol is freshly prepared as for the fabrication of SAMs, no disulphide oxidation products are present according to NMR and MS analysis. In order to test the feasibility of the silyl ether cleavage, **7** was submitted to standard deprotection conditions using TBAF (Scheme 1) to quantitatively deliver the OH-free mannoside **8** (for ¹H-NMR cf. SI).

In view of the high yields and selectivities of the described reactions, the thiohexyl-modified azobenzene mannoside **7** appears as an ideal molecule for testing the concept of self-dilution to facilitate photoisomerization of SAMs (see below).

FULL PAPER for Chem. Eur. J.



For the fabrication of rigid SAMs, the molecules depicted in Figure 2 were targeted. The two mannosides differ in the arrangement of the biphenyl and the azo moiety relative to the sugar head group. A third azobenzene derivative was required as less bulky, though photoswitchable diluter molecule (see below). Figure 2 exemplifies the employed modular synthetic approach, where in each case complementary aryl iodides and arylboronic esters could be cross-coupled in a Suzuki reaction.^[20] Furthermore, it was necessary to select an appropriate method to furnish the free arylthiol functional groups. It turned out that the Newman-Kwart rearrangement could be successfully employed, in which *O*-thiocarbamates are thermally rearranged to *S*-thiocarbamates by intramolecular aryl migration. The latter can be readily hydrolysed under basic conditions to deliver the required thiophenols.

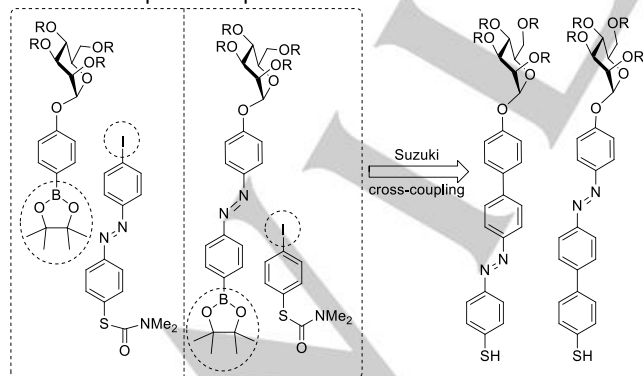
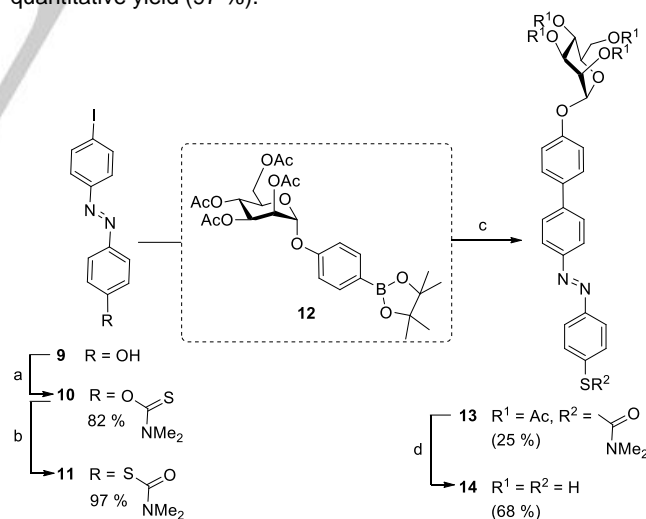


Figure 2. A modular synthesis delivers the target molecules (right) for the fabrication of rigid SAMs, employing the respective aryl iodides and arylboronic esters (boxed on the left) in Suzuki cross-coupling. *S*-thiocarbamates were derived from the respective *O*-thiocarbamates by Newman-Kwart rearrangement and served as precursors of the required aromatic thiols.

The photoswitchable mannoside **14** (Scheme 2) was selected as first target molecule for the rigid SAM approach. For its synthesis, commercially available iodo hydroxyazobenzene **9** was reacted with dimethylthiocarbamoyl chloride and DABCO as non nucleophilic base to give **10** in very good 82 % yield. In the following Newman-Kwart rearrangement, the *S*-thiocarbamate **11** was formed under solvent-free conditions at 200 °C in almost quantitative yield (97 %).



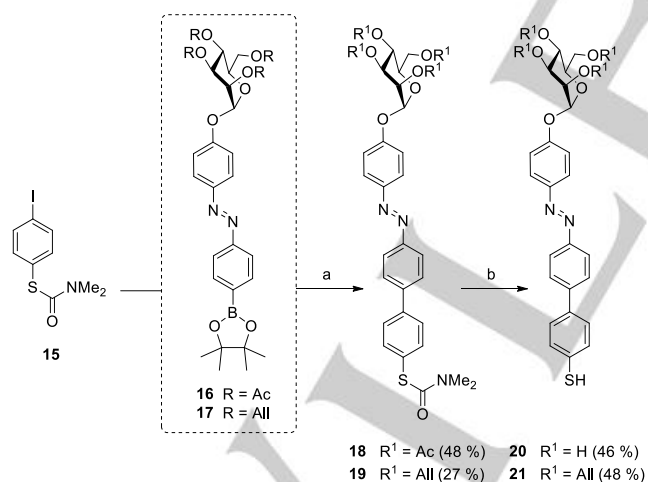
Scheme 2. Synthesis of the rigid *p*-mannosyloxyphenyl-azobenzene derivative **14**. Reagents and conditions: a) DABCO, dimethylthiocarbamoyl chloride, DMF, 5 h, 70 °C; b) 200 °C, 3 h; c) K₂CO₃, TBABr, Pd(PPh₃)₄, toluene, H₂O, 4 h, 80 °C; d) KOH, MeOH, 16 h, rt. DABCO: 1,4-diazabicyclo[2.2.2]octane; TBABr: tetrabutylammonium bromide.

FULL PAPER for Chem. Eur. J.

In the penultimate step of the synthesis, the iodoazobenzene **11** was subjected to a Suzuki coupling with the literature-known boronic ester **12**^[21] in order to introduce the α -D-mannopyranoside head group. This palladium-catalysed reaction was performed in a biphasic solvent mixture with tetrabutylammonium bromide (TBABr) as phase-transfer catalyst and delivered the protected mannoside **13** in a moderate yield of 32 %. The final deprotection step under basic conditions removed the *O*-acetyl protecting groups and delivered the free arylthiol at the same time to furnish the target molecule **14**.

As an alternative to **14** exhibiting a biphenyl spacer “above” the N=N group, mannoside **20** was synthesized, where the biphenyl spacer is positioned “below” the N=N moiety. To this end, the *S*-thiocarbamate **15**^[22] and the mannosyloxyazobenzeneboronate ester **16** or **17**, respectively, were submitted to the Suzuki reaction to yield the desired cross-coupling products, **18** or **19**, respectively, in fair yields. The boronates carrying different sugar protecting groups were obtained from the respective literature-known aryl iodides in high yield (cf. SI). Here, the chosen synthetic route provides an advantageous flexibility with respect to the variation of the sugar head group.

The Newman-Kwart rearrangement delivers the target mannoside **20** with the free arylthiol group starting from the *O*-acetylated analogue **18**. The *O*-allylated derivative **19** leads to **21** under the same reaction conditions (Scheme 3). We were interested to investigate the influence of the sugar protecting groups on the photoswitchability of SAMs fabricated from these molecules. The OH-unprotected mannosides are rather hydrophilic in comparison to their protected analogues, where *O*-acetylation leads to more electron-deficient glycosides in contrary to their *O*-allylated analogues.

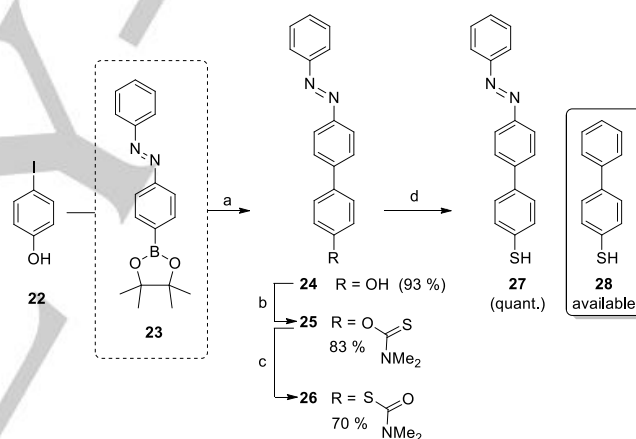


Scheme 3. Synthesis of the rigid *p*-mannosyloxy-*p'*-phenyl-azobenzene derivatives **20** and **21**. Reagents and conditions: a) Pd(PPh₃)₄, K₂CO₃, TBABr, toluene, H₂O, 16 h, 90 °C; b) KOH, MeOH, 1-2 h, reflux. TBABr: tetrabutylammonium bromide.

In order to modify SAMs formed from the *p*-mannosyloxy-*p'*-phenyl-azobenzene derivatives **20** as mixed SAMs, the azobenzene derivative **27** was prepared as photoswitchable

diluter molecule (Scheme 4). Included into SAMs, it can provide space for the mannose head groups but at the same time it can exhibit π - π -interactions in the backbone of the SAM. Because we were not satisfied with the yields obtained in the Suzuki cross-coupling reactions, we tried various catalysts to improve the yields of this reaction. For the synthesis of **24**, bis(2-amino-4,6-dihydropyrimidine)palladium(II)diacetate was synthesized from palladium acetate^[23] and used for the coupling of **22** and **23**.^[24] Indeed, this gave the biphenyl azobenzene **24** almost quantitatively.^[25]

Unfortunately, the same catalyst and reaction conditions did not lead to improvement of the yields for the mannoside analogues (cf. Schemes 2 and 3). After reaction of **24** with dimethylthiocarbamoyl chloride and sodium hydride, the *O*-thiocarbamate **25** was obtained and subsequently heated for 15 minutes at 270 °C in a Kugelrohr distillation apparatus to give the rearranged *S*-thiocarbamate **26** in a good yield. In this case, the rearrangement step was sensitive as longer reaction times resulted in low yields or even decomposition. As before, the free SH-group was furnished with an excess of KOH to give the diluter molecule **27**, to be compared with commercially available 4-biphenylthiol (**28**) (see below).



Scheme 4. Diluter molecules **27** and **28** for fabrication of mixed SAMs. Reagents and conditions for the synthesis of **27**: a) bis(2-amino-4,6-dihydropyrimidine)palladium(II)diacetate, MeOH, Na₂HPO₄, 2 h, 60 °C; b) NaH, dimethylthiocarbamoyl chloride, DMF, 24 h, 98 °C; c), 270 °C, 15 min; d) KOH, MeOH, 2 h 70 °C.

Prior to SAM fabrication and the investigation of their photoswitchability, the switching properties of the synthesized compounds were investigated in homogeneous solution (cf. SI). The photostationary states (PSS) and the half-lives associated with the thermal *cis*→*trans* relaxation were determined by NMR spectroscopy (cf. Table S12). As the investigated azobenzene derivatives are soluble in different solvents, the comparability of the results is somewhat limited, but clearly all tested compounds, **7**, **8**, **14**, **20**, **21**, and **27**, can reversibly be photoswitched between their *cis*- and *trans*-forms in homogeneous solution. The determined half-lives of thermal *cis*→*trans* relaxation are in a usual range (12 to 15 h), with the exception of **20** and **27** which exhibit faster *cis*→*trans* relaxation (half-lives < 2 h).

FULL PAPER for Chem. Eur. J.

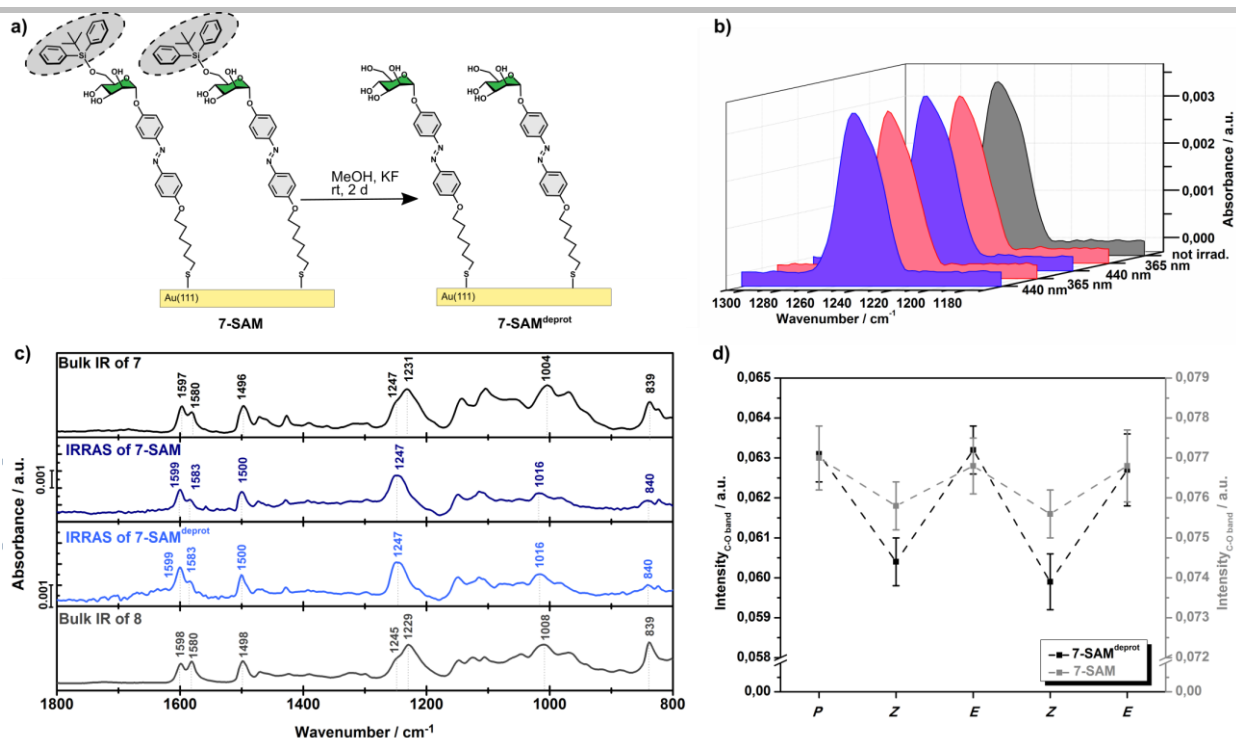


Figure 5. Vibrational data of compound **7** and **8**. a) Deprotection of the **7-SAM** with KF leads to the **7-SAM^{deprot}**. b) This display shows the reversibility of the *cis/trans*-isomerization of the **7-SAM^{deprot}** by means of the $C_{\text{aryl}}\text{-O}$ -stretch intensity after irradiation with light of 365 nm or 440 nm c) The measured bulk IR of compound **7** before and after the deprotection (**8**) and the IRRAS spectra of compound **7** in a monolayer on Au(111) before and after the cleavage of the TBDPS group (**7-SAM^{deprot}**). d) Comparison of the switching behavior before (**7-SAM**, grey) and after (**7-SAM^{deprot}**, black) the cleavage of the TBDPS group.

Infrared reflection absorption spectroscopy

The SAM of **7** (Figure 5, a) and its switching behavior were further investigated employing infrared-reflection-absorption-spectroscopy (IRRAS). Intensities of around 10^{-3} absorbance units are compatible with the formation of a monolayer on Au(111) (Figure 5, c).^[14] Notably, the different relative intensities in the measured bulk and surface IR spectrum, in particular in the regions around 1600 and 1200 cm^{-1} , are caused by the surface selection rule.^[32] Such differences are a first hint for a well-organized monolayer and a preferred orientation of the molecules on the surface.

The measured IR spectra were compared to calculated bulk IR spectra in order to designate the bands to specific vibrational modes. The IRRAS spectrum of the **7-SAM** shows several significant bands in the fingerprint region. The bands around 1600 cm^{-1} correspond to $C_{\text{aryl}}\text{-C}_{\text{aryl}}$ stretching vibrations of the azobenzene unit. A combination of the $\text{N}=\text{N}$ stretching and aromatic $\text{C}-\text{C}$ stretching vibration is located at 1498 cm^{-1} . The most prominent vibration at 1247 cm^{-1} can be assigned to the $C_{\text{aryl}}\text{-O}$ stretching vibration of the glycosidic oxygen. Importantly, the transition dipole moment of this vibrational mode is parallel to the axis of the azobenzene unit in the *trans*-state. Therefore, the transition dipole moment of this vibration shows the same orientation with respect to surface normal as the azobenzene unit in the SAM. Moreover, the orientation of this vibration changes during the isomerization of the azobenzene $\text{N}=\text{N}$ double bond. This, in turn, directly influences the intensity of the band in

the surface IR spectrum because of the surface selection rule.^[32] The $C_{\text{aryl}}\text{-O}$ vibration thus is well suited to monitor the *cis/trans*-isomerization of the glyco-SAMs adsorbed on Au(111) with IRRAS.^[6]

In order to detect the isomerization process with high sensitivity PM-IRRAS (polarization-modulated-IRRAS) in the spectral range of the $C_{\text{aryl}}\text{-O}$ vibration was applied. Due to the presence of a small shoulder in the investigated IR band ($C_{\text{aryl}}\text{-O}$ stretching vibration) at lower wavenumbers, the band was fitted with two Gaussians to determine the intensity of the pure $C_{\text{aryl}}\text{-O}$ band (see SI, Figure S14-S19). The second band corresponds to a $\text{C}-\text{H}$ bending vibration within the mannose moiety. This vibration is a combination of different vibrational modes. Moreover, the mannose moiety can rotate around the anomeric $\text{C}-\text{O}$ bond. For this reason, the intensity of this band is barely affected by the isomerization process and can be considered as constant. The change of the $C_{\text{aryl}}\text{-O}$ bond orientation was calculated by geometry optimizations of the *cis*- and *trans*-isomer (see SI, Figure S22). For the *cis*-isomer a CNNC angle ($C_{\text{aryl}}\text{-N}_{\text{azo}}\text{-N}_{\text{azo}}\text{-C}_{\text{aryl}}$) of 69.4° was obtained while it is 179.9° for the *trans*-isomer. Thus CNNC angle change γ amounts to 110.5° during the isomerization reaction (cf Figure 4), a result which fits well to data of pure azobenzenes reported in the literature.^[33] Nevertheless, only small changes ($\Delta I_{\text{exp.}}=2\%$) of the $C_{\text{aryl}}\text{-O}$ stretch intensity are observed upon irradiation of **7-SAM** adsorbed on gold with light of 365 nm (Figure 5, d; see SI, Figure S16).

FULL PAPER for Chem. Eur. J.

Taking the tilt angle β determined by NEXAFS into account, the angle φ between the transition dipole moment of the $C_{\text{aryl}}\text{-O}$ stretching vibration and the surface normal can be determined. However, whereas for *trans* $\varphi_{\text{trans}}=\beta$, there are several possibilities for *cis*; i.e., the azo group can isomerize towards the surface ("into" the SAM, A) or into a configuration more parallel to the surface ("onto" the SAM, B; $\varphi(\text{A})_{\text{cis}}=180^\circ-\gamma-\beta$, $\varphi(\text{B})_{\text{cis}}=\gamma-\beta$; Figure 4). Moreover, an equal distribution of all transition-dipole orientations within these two extremes; i.e., within a corresponding cone around the molecular axis, is theoretically possible (Figure 4, C). In this case, a rotational averaging over all possible azimuthal angles has to be performed (see Experimental section). Although, due to steric reasons, a preferential orientation of the head group (e.g., B) might exist in the *cis*-configuration of the investigated glyco-SAMs, this question cannot be decided without further information. In view of this situation we thus compare ΔI_{exp} values based on IRRAS data with ΔI_{theo} values obtained from orientation A (head group towards the surface), B (head group approx. parallel to the surface) and C (rotational average) in Table 1. Based on C, an intensity decrease of $\Delta I_{\text{theo}}=71\%$ is predicted if all molecules in the **7-SAM** switch to the *cis*-isomer. The observed intensity change ($\Delta I_{\text{exp}}=2\%$) thus would indicate that only 3% of molecules switch to the *cis*-isomer (Table 1). Taking the steric demand of the TBDPS group into account, this result is consistent with previous studies^[6] on pure glyco-SAMs.

In order to increase the free volume for the *trans*→*cis* isomerization of surface-adsorbed compound **7** the protection group was cleaved off by immersing the functionalized substrate into a solution of potassium fluoride in methanol for two days (Figure 5, a). Resulting **7-SAM^{deprot}** (after on-surface cleavage of the TBDPS group) was again investigated by XPS, NEXAFS and IRRAS to evaluate its switching behavior. Except for small changes in intensity, the surface IR spectrum, shown in Figure 5 (c), exhibits no large differences between the protected and deprotected SAM of compound **7** on Au(111). This result is compatible with the similarity of the bulk spectrum of **7** and the bulk spectrum of **8** obtained from deprotection of **7** in homogeneous solution (Figure 5, c).

In contrast to the vibrational spectra, the XPS data (see SI, Figure S1) clearly reflect the successful deprotection reaction on the surface; i.e., the signal in the Si 2p region becomes significantly smaller. These data suggest that most of the TBDPS groups were in fact cleaved by the treatment of the functionalized substrate with potassium fluoride. At the same time the SAM stayed intact according to the S 2p spectrum, which even after on-SAM deprotection (see SI, Figure S1) still prominently exhibits the thiolate species. The orientation of **7-SAM^{deprot}** was again elucidated by NEXAFS. Remarkably, after the on-surface deprotection the tilt angle β still amounts to $33\pm 2^\circ$ ($\Delta I_{\text{theo}}=69\%$, based on orientation C), very similar to the original value (see SI, Figure S12). This underscores the conformational stability of **7-SAM**, which maintains its original orientation even after cleavage of the TBDPS groups on SAM.

After deprotection, the intensity change due to the *trans/cis*-isomerization increases significantly ($\Delta I_{\text{exp}}=5\%$; Figure 5, b and d). Based on the rotationally averaged *cis*-configuration C, this intensity change indicates that 7% of the molecules on the surface switch to the *cis*-isomer, corresponding to an increase of the switching capability of more than 100% with respect to the original **7-SAM**. The performance of the self-diluting SAM thus is superior to results of alkyl-based glyco-SAMs, the maximum switching capacity of which (using a diluter compound) was 4%.^[6] In Figure 5 (b, d) it is also shown that the *cis/trans*-isomerization is fully reversible. By alternating irradiation with light of 440 nm and 365 nm it was possible to switch the glyco-SAM back and forth with a constant intensity change of $\Delta I_{\text{exp}}=5\%$ (see SI, Figure S17). Interestingly, if compound **7** was deprotected in solution and subsequently deposited on the surface, the resulting **8-SAM** (deprotection in solution before surface deposition) showed only very weak changes ($\Delta I_{\text{exp}}<1\%$) in the intensity of the $C_{\text{aryl}}\text{-O}$ -vibration after irradiation with light of 365 nm (see SI, Figure S20). This indicates that the improvement of the switching behavior is only observed if the TBDPS protection group is cleaved on the surface and underlines the feasibility of the self-dilution concept towards photoswitchable SAMs.

Table 1. Comparison of the switching behavior of the investigated glyco-SAMs. β is the tilt angle with respect to the surface normal. The angle φ describes the orientation of the transition dipole moment of the $C\text{-O}_{\text{aryl}}$ stretching vibration in the *cis*-isomer with respect to the surface normal. A and B describe the two extrema from Figure 4. The value ΔI_{theo} corresponds to the expected maximum intensity change of the $C\text{-O}_{\text{aryl}}$ stretching vibration considering β and the spatial change during the isomerization in dependence of the orientation of the *cis*-isomer within the glyco-SAM (A: head group downwards; B: head group upwards; C: average). ΔI_{exp} is the experimentally (IRRAS) obtained intensity change. By means of these values the switching capacity was calculated.

SAM	Tilt angle (β)	$\varphi(\text{A})_{\text{cis}}$	$\varphi(\text{B})_{\text{cis}}$	ΔI_{theo} based on orientation A	ΔI_{theo} based on orientation B	ΔI_{theo} based on averaged orientation C	Experimental change of intensity (ΔI_{exp})	Switching capacity ($\Delta I_{\text{exp}}/\Delta I_{\text{theo}}$) based on C	Reversibility
7-SAM	$32\pm 2^\circ$	$38\pm 2^\circ$	$79\pm 2^\circ$	14 %	94 %	71 %	2 %	3 %	yes
7-SAM^{deprot}	$33\pm 2^\circ$	$37\pm 2^\circ$	$78\pm 2^\circ$	11 %	94 %	69 %	5 %	7 %	yes
8-SAM	---	---	---	---	---	---	<1 %	---	---
20-SAM	$23\pm 6^\circ$	$47\pm 6^\circ$	$88\pm 6^\circ$	45 %	99 %	80 %	27 %	34 %	no
20,27-SAM	$22\pm 2^\circ$	$48\pm 2^\circ$	$89\pm 2^\circ$	47 %	99 %	80 %	38 %	48 %	yes
20,28-SAM	$24\pm 3^\circ$	$45\pm 3^\circ$	$87\pm 3^\circ$	41 %	99 %	78 %	18 %	23 %	yes
21-SAM	$24\pm 5^\circ$	$45\pm 5^\circ$	$87\pm 5^\circ$	41 %	99 %	78 %	9 %	12 %	yes
14-SAM	$29\pm 3^\circ$	$40\pm 3^\circ$	$81\pm 3^\circ$	24 %	97 %	73 %	5 %	7 %	no

[^{deprot}] = on-surface cleavage of the TBDPS group.

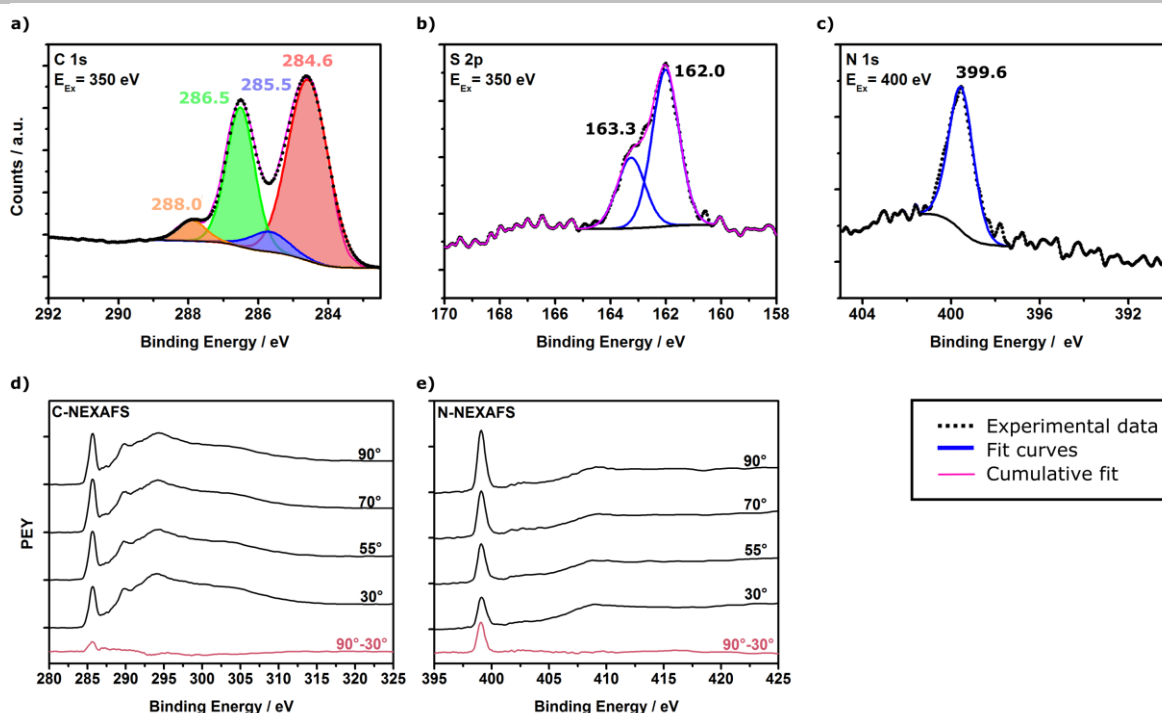


Figure 6. XP spectra and normalized NEXAFS spectra at different angles of **20-SAM** adsorbed on Au(111). The C 1s (a), S 2p (b) and N 1s (c) are shown. The baseline is shown in black, the measured data are represented by black dots and the fitted sum spectrum is illustrated by the magenta line. The C K-edge spectrum (d) and the N K-edge spectrum (e) are shown. The difference spectra (90° - 30°) are shown in red.

3. Surface spectroscopic investigation of rigid glyco-SAMs

For the fabrication of rigid glyco-SAMs, the azobenzene mannosides **14**, **20**, and **21** were employed. They were deposited on Au(111) from a methanol/acetone (95:5) solution, and the resulting monolayers on Au(111) were investigated with XPS, NEXAFS and IRRAS.

X-ray photoelectron spectroscopy

The XPS data of the **20-SAM** are shown in Figure 6. The C 1s spectrum (Figure 6, a) contains three different signals. The main component at 284.6 eV (59 %, red) can be assigned to the aromatic carbon atoms bound to each other or to sulfur. A smaller signal at 285.5 eV (7 %, blue) corresponds to the carbon atoms bound to nitrogen. The third species (29 %, green) at 286.5 eV can be associated with carbon atoms bound to oxygen. The anomeric carbon atom which is bound to two oxygen atoms contributes to a fourth signal at 288.0 eV (5 %, orange). Again, the relative fractions of the different species fit well to the chemical composition (62:8:25:5) of compound **20**. The S 2p spectrum (Figure 6, b) exhibits only one doublet at 162.0 eV and 163.3 eV (100 %, red), corresponding to a thiolate species.^[28–30] Importantly, there is no disulfide or other sulfur containing impurity detectable. This clearly reflects the high purity of the

SAM and furthermore proves the covalent attachment of the molecule to the surface. Also the N 1s spectrum shows only one component (100 %, blue) at 399.6 eV which corresponds to the azo moiety of the **20-SAM** (Figure 6, c).^[6,26,27] In conclusion, the XP spectra confirm the presence of a monolayer of compound **20 (20-SAM)** in high purity.

Near-edge X-ray absorption fine structure spectroscopy

NEXAFS spectra were measured at the carbon and nitrogen K-edges for monolayers of azobenzene mannoside **20** on Au(111) single crystals. The carbon K-edge spectrum, shown in Figure 6 (d), exhibits a prominent resonance at 285.4 eV which can be assigned to a $1s \rightarrow \pi^*$ (LUMO) transition. This resonance reveals a decreasing intensity from 90° to 30° . The second π^* resonance is located at 287.4 eV and shows almost no angular dependence, just as the third π^* resonance at 298.7 eV. At higher energies (293.8 eV) several broadened σ^* resonances can be observed.

The nitrogen K-edge NEXAFS in Figure 6 (e) reveals one prominent resonance at 399.0 eV. The energy of this feature again corresponds to the N 1s-to- π^* -transition reported in literature for azobenzene units.^[27] The difference spectrum (red) shows that this transition exhibits a marked angular dependence. The tilt angle β of the compound **20** with respect to the surface normal amounts to $23 \pm 6^\circ$ (see SI, Figure S12) which fits well to results of other biphenyl based SAMs in literature.^[34] This result is in accordance with the carbon K-edge NEXAFS data.

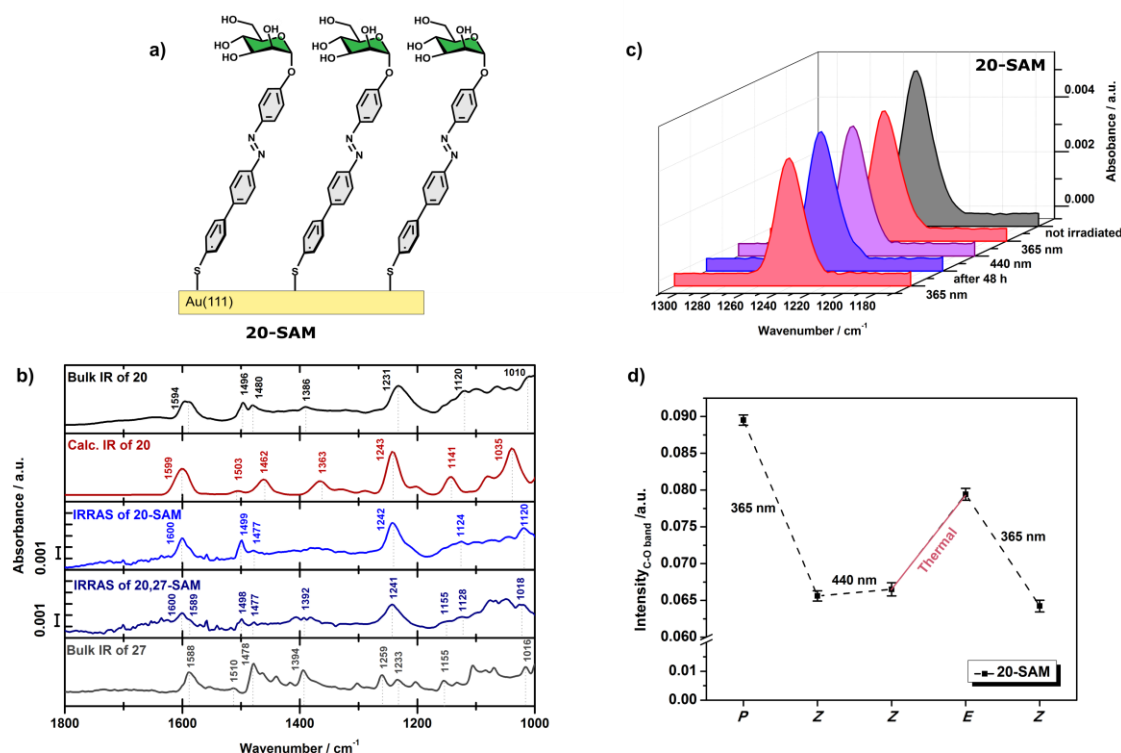


Figure 7. a) Schematic illustration of compound **20** in a monolayer on Au(111); b) Measured bulk IR of **20** (black) and **27** (grey) and IRRAS spectra of the **20-SAM** (blue) and the **20,27-SAM** (marine blue) in comparison with the computed bulk IR (red) of compound **20**. c) PM-IRRAS spectra in the $C_{aryl}-O$ region of the **20-SAM** before (grey) and after irradiation with light of 365 nm (red), followed by irradiation at 440 nm (purple); spectrum after thermal relaxation (blue); d) Intensity of the $C_{aryl}-O$ stretching vibration after irradiation with light of 365 nm, followed by irradiation at 440 nm and thermal relaxation for the **20-SAM**.

Infrared reflection absorption spectroscopy

Besides XPS and NEXAFS, IRRAS was employed to investigate compound **20** adsorbed as a monolayer on Au(111), in particular its switching properties. Intensities of around 10^{-3} absorbance units again reflect the formation of a monolayer on Au(111) (Figure 7, a).^[14] The measured bulk IR and IRRAS spectra look very similar to the calculated bulk IR spectrum. With the help of the calculated spectrum the bands appearing in the measured spectra can be assigned to specific vibrational modes. The vibrational mode at 1600 cm^{-1} in the IRRAS spectrum corresponds to $C_{aryl}-C_{aryl}$ stretching vibrations of the biphenyl unit. In the IRRAS spectrum the bands at 1499 cm^{-1} and 1477 cm^{-1} exhibit a different intensity ratio than in the bulk IR due to the surface selection rule.^[32] These vibrations can be assigned to N=N stretching and aromatic C-C stretching vibrations, respectively.

At 1242 cm^{-1} in the surface IR and at 1231 cm^{-1} in the bulk IR spectrum the very prominent $C_{aryl}-O$ stretching vibration can be observed (Figure 7, b). In analogy to **7-SAM** described above this vibration is well suited to monitor the *cis/trans*-isomerization of **20-SAM** with PM-IRRAS.^[6] The first measurement (grey in Figure 7c) shows the spectrum of the un-irradiated sample. After irradiation with light of 365 nm the intensity of the $C_{aryl}-O$ vibration decreases by $\Delta I_{exp}=27\%$ (red) (Figure 7d). This reflects the *trans* \rightarrow *cis* isomerization of the **20-SAM** and the corresponding orientational change of the transition dipole moment of the $C_{aryl}-O$ stretch. The possible orientations of the $C_{aryl}-O$ stretch in the *cis*-isomer were determined in analogy to the azobenzene mannosides **7** and **8**

with a flexible backbone (see above). Based on the rotationally averaged *cis*-configuration C, a decrease of $\Delta I_{theo}=80\%$ of the $C_{aryl}-O$ intensity is predicted. From the observed intensity decrease it thus can be concluded that more than one third of the molecules (34 %) in the **20-SAM** switch to the *cis*-isomer (Table 1). Remarkably, the switching capacity of **20-SAM** thus exceeds that obtained for SAMs formed of compounds **7** and **8** by almost one order of magnitude.

In order to switch *cis-20-SAM* back to the *trans*-isomer, the sample was irradiated with light of 440 nm wavelength. Surprisingly, no increase of the $C_{aryl}-O$ stretch intensity was observed (Figure 7, c and d). Thus, it was concluded that it is not possible to photochemically switch the SAM back to the *trans*-configuration. However, after leaving the sample for 48 h at room temperature and under N_2 -atmosphere a slight increase (+ 8 % intensity) of the $C_{aryl}-O$ band could be observed, which was attributed to a thermal relaxation process. This small amount of *trans*-isomer, in turn, could be switched back to the *cis*-state by irradiation with light of 365 nm.

The described results indicate a high thermal stability of *cis-20-SAM* on Au(111). Since similar SAMs devoid of a sugar head group show reversible *cis/trans*-isomerization,^[16] we assume intermolecular interactions within the SAM as a possible origin for this observation. Hydrogen bonds of the D-mannose head group of the SAM, could stabilize the *cis*-isomer on the surface and prevent *cis* \rightarrow *trans* back isomerization. In order to check such an effect of the free hydroxy groups of the sugar ring, the O-allylated analogue of **20**, the mannoside **21** was employed and

FULL PAPER for Chem. Eur. J.

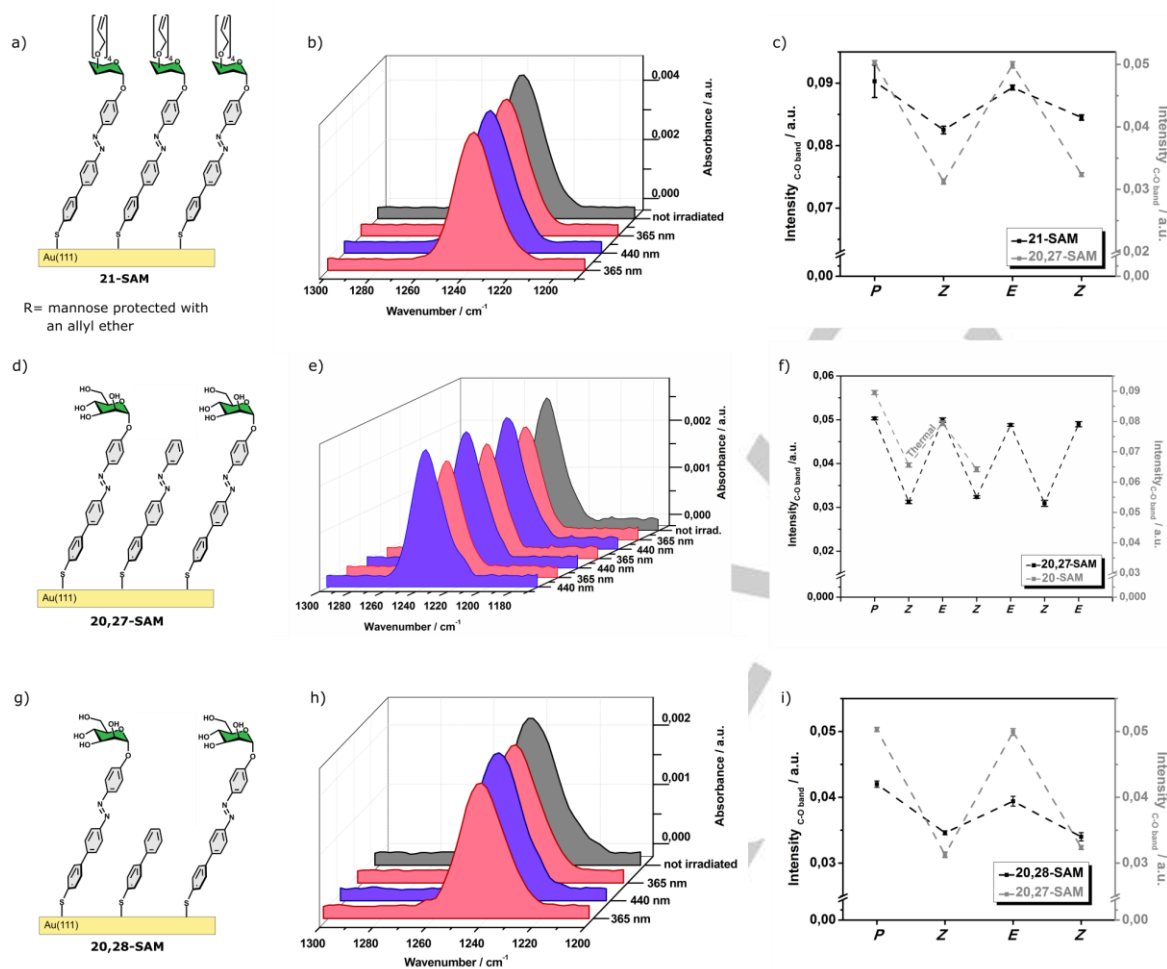


Figure 8. a) Schematic illustration of the **21-SAM**. b) PM-IRRA spectra of the $C_{\text{aryl-O}}$ region of the **21-SAM** before and after irradiation with light of 365 nm and 440nm. c) The changes of the intensities of the $C_{\text{aryl-O}}$ stretching vibration after irradiation with light of 365 nm or 440 nm for the **21-SAM** (black) in comparison with the data of the **20,27-SAM** (grey). d) Schematic illustration of the **20,27-SAM**. e) PM-IRRA spectra of the $C_{\text{aryl-O}}$ region of the **20,27-SAM** before and after irradiation with light of 365 nm and 440nm. f) The changes of the intensities of the $C_{\text{aryl-O}}$ stretching vibration after irradiation with light of 365 nm or 440 nm for the **20,27-SAM** (black) in comparison with the data of the pure **20-SAM** (grey). g) Schematic illustration of the **20,28-SAM**. h) PM-IRRA spectra of the $C_{\text{aryl-O}}$ region of the **20,28-SAM** before and after irradiation with light of 365 nm and 440 nm. i) The changes of the intensities of the $C_{\text{aryl-O}}$ stretching vibration after irradiation with light of 365 nm or 440 nm for the **20,28-SAM** (black) in comparison with the data of the **20,27-SAM** (grey).

deposited % and for comparison, 8-SAM which showed almost no *trans/cis* switching on surface on a Au(111) surface from a 1 mM methanol/acetone (95:5) solution. The obtained film was investigated by XPS, NEXAFS and IRRAS (see SI, Figure S4 & S10 & S19), providing evidence for a highly pure and well-oriented monolayer of **21** on Au(111). The tilt angle β of the molecules within the **21-SAM** was found to be $24 \pm 5^\circ$ ($\Delta I_{\text{theo.}} = 78\%$ based on the orientationally averaged *cis*-configuration C), quite similar to parent **20-SAM**. The switching properties of the **21-SAM** were elucidated with PM-IRRAS; the resulting spectra are shown in Figure 8 (a-c). By irradiation of the sample with light of 365 nm the intensity of the $C_{\text{aryl-O}}$ stretching vibration decreases by $\Delta I_{\text{exp.}} = 9\%$. Again, this intensity change can be attributed to the *trans/cis*-isomerization of compound **21** adsorbed on the surface. After irradiation with light of 440 nm the intensity rises again. The switching capacity calculated on the basis of $\Delta I_{\text{exp.}}$ and $\Delta I_{\text{theo.}}$ amounts to 12 %. Consequently, this process is reversible for **21-SAM** (Figure 8, a-c), in contrast to parent **20-SAM**. However, the

change of intensity is noticeably lower than for the original **20-SAM**.

From the described results we conclude that the free OH-groups of the mannose head groups of **20-SAM** stabilize the *cis*-isomer on the surface *via* intermolecular hydrogen bonds, preventing the molecules to be switched back to the *trans*-state by irradiation with 440 nm light. Otherwise, when the hydroxy groups are protected, stabilization of the *cis*-isomer by H-bonds is no longer possible and the switching process becomes reversible. On the other hand, the steric demand of the head group is drastically increased by four allyl protection groups which lowers the free volume within the SAM. For this reason the switching capacity of the **21-SAM** is distinctly lowered in comparison to the **20-SAM**.

In addition to the rigid *p*-mannosyloxy-*p'*-phenyl-azobenzene derivative **20** and its protected analogue **21**, the isomeric glycoazobenzene derivative **14** was tested, where the azobenzene moiety is shifted one phenyl group away from the

FULL PAPER for Chem. Eur. J.

sugar ring, leading to a *p*-mannosyloxyphenyl-azobenzene structural motive (cf Scheme 2). A monolayer of this molecule was deposited on gold and investigated by XPS, NEXAFS and IRRAS as before (see SI, Figure S5 & S11 & S21). The tilt angle of the **14-SAM** with respect to the surface normal was determined to $\beta=29\pm 3^\circ$ ($\Delta I_{\text{theo}}=73\%$, based on configuration C). Upon irradiation with light of 365 nm and 440 nm a reversible change of $\Delta I_{\text{exp}}=5\%$ could be observed for the $C_{\text{aryl}}\text{-O}$ stretching vibration intensity, corresponding to a switching capacity of 7 % for **14-SAM**. The much lower value compared to **20-SAM** (34 %) and **21-SAM** (12 %) can be explained by the large free volume required for the reorientation of the mannosyloxybiphenyl moiety "above" the azo group as compared to the shorter mannosylphenyl portion which terminates **20-SAM**. This result demonstrates that the biphenyl group should be placed *below* (and not *above*) the azo function to obtain a satisfactory switching behavior of the respective glyco-SAM on a Au(111) surface.

Investigation of mixed rigid SAMs

In order to increase the lateral distance between the head groups and reduce their intermolecular interactions, **20-SAM** was diluted with the azobenzene derivative **27** lacking the mannose unit. Mixed SAMs were fabricated by immersing the substrate in a solution containing both compounds, the diluter molecule **27** and **20** in a ratio of 4:1, which was found optimal in our earlier studies with diluted SAMs.^[6] Moreover, it is known that the ratio of components assembled in a SAM is not necessarily the same as in the solution used for immersion of the gold wafer.^[10]

To check the purity, composition and orientation of the mixed **20,27-SAM**, XPS and NEXAFS measurements were conducted (see SI, Figure S2 & S8). The composition in the C 1s XP spectrum reflects a 1:1-ratio of compound **20** and **27** in the surface-adsorbed SAM. This agrees with the observation that the intensity of the $C_{\text{aryl}}\text{-O}$ stretching vibration in the surface IR spectrum is reduced by about 50 % (Figure 7a). The NEXAFS data of the **20,27-SAM** and the pure **20-SAM** are almost equal, because the most intense NEXAFS resonances originate from the benzene and azo units of the molecules. This suggests that the dilution of the SAM does not influence the orientation of the molecules. The tilt angle β of the **20,27-SAM** with regard to the surface normal determined by NEXAFS is $22 \pm 4^\circ$ ($\Delta I_{\text{theo}}=80\%$, based on orientation C). The IRRAS spectrum of the mixed **20,27-SAM** in Figure 7 (a) still shows the same vibrations like in the pure **20-SAM**. This is reasonable, since the structure of diluter molecule **27** is very similar to that of its glycosylated analogue **20**. The $C_{\text{aryl}}\text{-O}$ stretching vibration is still very prominent, but less intense compared to the pure **20-SAM**. In addition, at 1215 cm^{-1} a shoulder is observable which can be assigned to a C-N stretching vibration combined with a $C_{\text{aryl}}\text{-C}_{\text{aryl}}$ stretching vibration of the azobenzene in the diluter molecules.

In order to investigate the switching behavior of the mixed **20,27-SAM**, PM-IRRAS was employed in the spectra region of the $C_{\text{aryl}}\text{-O}$ stretch. After irradiation with 365 nm the intensity of the $C_{\text{aryl}}\text{-O}$ stretching mode decreases in the surface IR spectrum by $\Delta I_{\text{exp}}=38\%$ due to the *trans/cis*-isomerization and the associated change in orientation with respect to the surface (see SI, Figure S15). This corresponds to a switching capacity of 48 %, even larger than observed for pure **20-SAM**; i.e., nearly the half of the molecules (48 %) in the **20,27-SAM** have been switched from the *trans* to the *cis* state. Moreover, as shown in Figure 8 (d-f), this

process is fully reversible. Thus, by dilution of **20-SAM** with compound **27** a reversible *cis/trans* isomerization of this glyco-SAM is enabled.

In a final step, a different diluter compound was employed than in the **20,27-SAM**, in order to check the influence of a comprised azobenzene unit (as in **27**) on the switching properties of a mixed glyco-SAM. To this end, 4-biphenylthiol (**28**, cf. Scheme 4) was employed as non photoswitchable diluter molecule, and a **20,28-SAM** on Au(111) was prepared. The sample was deposited from a 1 mM solution of compounds **20** and **28** (1:4) in a methanol-acetone mixture (95:5). The XPS, NEXAFS and IRRAS data prove that the SAM is of high purity and that the composition of the **20,28-SAM** is again 1:1 (see SI; Figure S3 & S9). The orientation of the **20,28-SAM** was determined by NEXAFS. With $24 \pm 3^\circ$ ($\Delta I_{\text{theo}}=78\%$, based on orientation C) the tilt angle is again very similar to that of **20-SAM** (see SI, Figure S12). In Figure 8 (g-i) the PM-IRRAS data of the **20,28-SAM** are shown. By irradiation of the sample with light of 365 nm the intensity of the $C_{\text{aryl}}\text{-O}$ stretching vibration decreases by $\Delta I_{\text{exp}}=18\%$. Even though this process is reversible, the switching behavior is significantly worse than for the pure **20-SAM** and mixed **20,27-SAM**. Thus, we conclude that the azobenzene moiety is an essential part of the diluter molecule to obtain efficient and reversible switching properties of the respective glyco-SAM.

4. Lectin binding tests

For a first biological evaluation of the effect of *trans/cis* isomerization of the new glyco-SAMs on carbohydrate recognition, the fluorescein-labeled lectin Concanavalin A (ConA-FITC) was used. For this well-known lectin, a strong specificity for $\alpha\text{-D}$ -mannosyl residues is known and hence it is suited for binding studies with the herein prepared SAMs. Three different monolayers were selected for the tests, the pure **20-SAM**, with a switching capacity of 34 % (cf. Table 1), its diluted version, **20,27-SAM**, which performed best among all investigated SAMs with a switching capacity of 48 %, and in addition **8-SAM** was tested, which showed almost no *cis/trans* isomerization on surface. The respective SAMs were subdivided into two halves and irradiated with light of 365 nm (to effect *trans*→*cis* isomerization) or 485 nm wavelengths (to effect *cis*→*trans* isomerization). Then the wafers were incubated with ConA-FITC and after washing, fluorescence of bound lectin was read out (cf. supporting information, Fig. S 84). Strikingly, lectin binding to **20-SAM** was reduced by 28 % after irradiation with light of 365 nm, whereas **20,27-SAM** after the same *trans*→*cis* isomerization step even showed 33 % reduced lectin binding compared to the *trans*-state of the SAM. These data parallel the determined switching capacities of the SAMs (34 % and 48 %) but also show that additional effects other than *trans*→*cis* isomerization add to carbohydrate recognition on a surface. This finding is not unexpected and might be interpretable in context of the tetrameric nature of ConA at pH higher than 6. Very much in line with the spectroscopic investigation, irradiation of **8-SAM** showed so significant effect on lectin binding. In future experiments, *cis/trans* isomerization of the so far available glyco-SAMs has to be investigated in different biological systems to advance our understanding of the biological effect of carbohydrate ligand orientation on surfaces.

FULL PAPER for Chem. Eur. J.

Conclusions

The switching capacity of glyco-SAMs is of fundamental importance for their biological function. Therefore, it has been our goal to design glycoazobenzene thiols for the fabrication of glyco-SAMs on Au(111) with high switching capacity. To this end, it was important to form stable SAMs and concomitantly provide enough free volume for the reversible *cis/trans* photoisomerization. We have varied central molecular parameters, in particular, protecting groups on the sugar ring and backbone rigidity of the immobilized molecules to investigate their influence on the physicochemical properties of the respective glyco-SAMs; in particular, their switching behavior.

Six new azobenzene mannosides were synthesized and characterized in bulk material and in solution, where all synthetic compounds show reversible *cis/trans* isomerization. Afterwards they were deposited on a Au(111) surface and the composition and packing density of the formed SAMs spectroscopically characterized with a combination of IRRAS and NEXAFS. XPS data were used to determine the chemical composition of the SAMs and proved the high purity of the investigated SAMs. It was also possible to verify the deprotection "on SAM" by the Si 2p region of XP spectrum. The molecular orientation of the SAMs with respect to the surface was determined by NEXAFS spectroscopy. For the alkyl SAMs a tilt angle β regarding to the surface normal between 32°-33° was obtained; for the rigid SAMs the tilt angle β was found between 22° and 24°. Both results fit well to previous studies in the literature.

The switching behavior of the glyco-SAMs was investigated with the help of IRRAS. Based on the intensity change of the $\text{C}_{\text{aryl}}\text{-O}$ stretching vibration upon *cis/trans*-isomerization and the orientation of the molecules obtained by NEXAFS, the switching capacities of the different glyco-SAMs were determined. The approach of self-dilution within the glyco-SAM leads to an improvement of the inherently low switching capacities by more than 100 % (**7-SAM**: 3 %; **7-SAM**^{deprot}: 7 %). Much higher switching capacities could be obtained using SAMs with rigid spacers. In pure **20-SAM** 34 % of the molecules switched from *trans*- to the *cis*-isomer due to irradiation with light of 365 nm. However, **20-SAM** could not be switched back to *trans*-state by irradiation with light of 440 nm. Here, only a slow thermal relaxation could be observed. By protecting the OH-groups of the mannose moiety the reversibility of the *cis/trans*-isomerization was restored (**21-SAM**), but under loss of switching capacity. In contrast, diluting the rigid SAMs was found to both improve the switching capacity and enable reversible switching. In **20,27-SAM** almost half of the molecules undergo a reversible *trans/cis* isomerization (48 %). These switching properties are unprecedented and mark a significant progress in the field of photoswitchable glyco-SAMs. It was found to be necessary that the diluter compound also contains an azobenzene, at the same position as in the glyco compound. Otherwise the switching capacity decreases sharply (**20,28-SAM**; 23 %). First lectin assays with ConA showed that the observed differences in lectin binding parallel with the switching capacities of the SAMs but that the determined lectin binding differences are smaller than the *cis/trans* ratios of the investigated SAMs.

In conclusion, this study provides new and detailed information about different approaches towards photoswitchable glyco-SAMs. Eventually, these surfaces have to be employed to

further improve the photoswitchability of cell adhesion compared to already established systems^[6,7] and to advance our understanding of the underlying effects.

Experimental Section**General procedures**

Chemicals were purchased from Sigma-Aldrich, Acros Organics, or TCI and were used without further purification. Moisture sensitive reactions were carried out in dry glassware and under positive pressure of nitrogen. Before adding tetrakis(triphenylphosphine)palladium(0), the reaction mixtures were degassed over three freeze-pump-thaw (F-P-T) cycles. Otherwise the flask with the reaction mixture was sonicated in an ultrasonic bath for 10 minutes. Thin layer chromatography was performed on silica gel plates (GF, 254, Merck). Visualization was achieved by UV and/or vanillin 10 % sulfuric acid in ethanol followed by heat treatment. Flash chromatography was performed on silica gel 60 (Merck, 230-400 mesh, particle size 0.040-0.063 nm) by using distilled solvents. Optical rotations were measured with a Perkin-Elmer 241 polarimeter (sodium D-line: 589 nm, length of cell: 1 dm) in the noted solvents. ¹H, ¹³C, ¹¹B NMR spectra were recorded with Bruker DRX-500 and AV-600 spectrometers. Chemical shifts were reported relative to internal tetramethylsilane or to the residual proton of the NMR solvent. All NMR spectra of the *E*-isomers of the azobenzene derivatives were recorded after they were kept for 16 h in the dark at 40 °C. IR spectra were measured with a Perkin Elmer FT-IR Paragon 1000 (ATR) or a Perkin Elmer Lambda 650 and were reported in cm⁻¹. Elemental Analyses were measured on a EuroEA 3000 from Euro Vektor and a vario MICRO cube from Elementar. The thermal *cis/trans*-isomerization was measured on a Bruker ARX 300 spectrometer.

Gold Substrates

Glass substrates with a 50 Å titanium adlayer and a 200 nm evaporated gold film from EMF corporation (Ithaca, NY) were used for IRRAS measurements. XPS and NEXAFS measurements were made with sputtered Au(111) single crystals.

Preparation of Monolayers

The monolayers of **7** and **8** were prepared by immersing Au(111) substrates in 0.5 mM solutions of the respective compound in methanol at room temperature. The monolayers of **14**, **20**, **21**, **27** and **28** as well as the respective mixed SAMs were prepared by immersing Au(111) substrates in 0.5 mM solutions of the respective compound in methanol/acetone (95:5) at room temperature. After 48 h of immersion the sample was removed from the solution, rinsed with methanol, acetone and dried in a stream of nitrogen gas.

IRRAS

The surface adsorbed molecules were investigated by using a Bruker VERTEX 70 FT-IR spectrometer equipped with a Polarization Modulation Accessory (PMA) 50 unit (Bruker Optik GmbH, Ettlingen, Germany). This instrument allows recording IRRAS and PM-IRRAS data with a spectral range from 4000 down to 800 cm⁻¹. IRRAS data were collected with a liquid nitrogen cooled MCT detector in a horizontal reflection unit for grazing

FULL PAPER for Chem. Eur. J.

incidence (Bruker A518). The sample chamber was purged with dry nitrogen before and during measurements. A deuterated hexadecane-thiol SAM on Au(111) was used as a reference for the background spectrum for conventional IRRAS spectra. Each spectrum contains 2048 averaged spectra. A p-polarized beam at an incident angle of 80° to the surface normal was used for measurements. All spectra were recorded with 4 cm⁻¹ resolution. PM-IRRAS data of the switching experiments were collected with the PMA 50 accessory using a liquid nitrogen-cooled MCT detector. The PEM maximum efficiency was set for the half-wave at 1750 cm⁻¹ for analysis of the area from 1400 cm⁻¹ to 1100 cm⁻¹. All spectra were recorded with 4 cm⁻¹ resolution.

Processing of IRRAS and PM-IRRAS data was carried out using the OPUS software Version 6.5 (Bruker, Germany). Baseline correction of the resulting IRRAS data was performed by the rubber band method in an interactive mode. PM-IRRAS data were processed by the implicit removal of the Bessel function through manual baseline correction. For the *trans/cis*-isomerization of different compounds adsorbed on Au(111) the prepared samples were irradiated within the spectrometer using a LED (Nichia NC4U133(T), peak wavelength: 365 (±9) nm or 440 (±5) nm, 1 LEDs, power dissipation: 12 W, luminous flux: 10 lm, distance ~5 cm). The sample was irradiated with the respective wavelength for 10 min.

Due to the small shoulder in the investigated IR band (C_{aryl}-O stretching vibration) at lower wavenumbers, the band was fitted with two Gaussians to determine the intensity of the C_{aryl}-O bond (see SI, Figure S14-S19). The second band corresponds to a C-H bending vibration within the mannose moiety. As this vibration is a combination of different vibrations and the mannose moiety can rotate around the C_{aryl}-O bond, the orientation of this vibration is only barely affected by the isomerization process and was thus neglected.

In order to calculate the expected intensity change ΔI_{theo} different orientations of the *cis*-isomer have to be taken into account, as the molecules within the SAM can rotate around their molecule axis. The orientations A (head group downwards) and B (head group upwards) were calculated based on the tilt angle β which was obtained from NEXAFS data. Using equation (1) and (2) the expected intensity change of the C_{aryl}-O stretch in the surface IR spectrum could be calculated:

$$\Delta I_{theo} = I_{trans}(1 - R_{theo}) \quad (1)$$

$$R_{theo} = \frac{\cos^2 \phi_{cis}}{\cos^2 \beta} \quad (2)$$

Since a distribution of orientations of the head group instead one specific orientation can be assumed within the glyco-SAM, another orientation was introduced called C. Orientation C describes an averaging over all possible angles of the transition dipole moment of the C_{aryl}-O stretch. The averaged intensity of the *cis*-isomer was calculated according equation (3):^[35]

$$\overline{I}_{cis} = \frac{1}{3} \left[\frac{1}{2} (3 \cos^2 \beta - 1) (3 \cos^2 (180 - \gamma) - 1) + 1 \right] \quad (3)$$

The angle γ corresponds to the angle between the molecule axis and the transition dipole moment of the C_{aryl}-O stretch in the *cis*-isomer.

XPS & NEXAFS

The XPS and NEXAFS measurements were performed at the BESSY II synchrotron radiation facility using the PREVAC endstation at the beamline HE-SGM. The experimental station is equipped with a hemispherical VG Scienta R3000 photoelectron

analyzer. The energy resolution E/DE of the beamline with 150 mm slits is 800. XP survey spectra were secured at 700 eV photon energy using an analyzer pass energy of 100 eV, whereas for the C 1s, Si 2p, and S 2p spectra the photon energy used was 350 eV with pass energy of 50 eV. For N 1s spectra the photon energy was at 500 eV with pass energy of 50 eV.

All spectra were acquired at normal electron emission. For determination of the relative composition of the adlayers, the XP spectra were energy-corrected using the Au 4f_{7/2} line at a binding energy of 84.0 eV as reference. Background correction was performed using a combination of a Shirley and a linear background for all signals. Peak fitting was performed using the program CASA XPS. The maximum deviation of fwhm of the fitted Gaussian within a spectrum was set to 0.2 eV. The fitting parameter are shown in Tables S1-S7 in the Supp. Inf. All spectra were smoothed with the SG Quadratic method (CASA XPS, smoothing width = 5) in order to improve the signal-to-noise-ratio. Care has been taken to ensure that this process does not alter the statement of the spectrum.

To correct for the photon flux of the NEXAFS measurements, all spectra were divided by the spectrum obtained for a freshly sputtered clean gold substrate and then edge-step normalized (using the average intensities for the C K-edge between 275 ± 0.5 eV and 320 ± 0.5 eV and for the N K-edge between 395 ± 0.5 eV and 420 ± 0.5 eV as pre- and post-edge). The normalized spectra were fitted employing a step function for the absorption edge and Gaussians for the π^* and σ^* resonances in order to determine the intensity I of specific resonances. In all spectra, the width of the step function was set to 0.2 eV. The series of spectra of a specific sample measured at different angles of incidence were fitted with the same parameter set, i.e., the energies of the resonances were allowed to vary in maximum by 0.2 eV and the half-widths at full maximum by 0.3 eV, as in agreement with the estimated experimental resolution. For determination of the orientation of the molecular orbitals, the angular dependence of the intensities I of the π^* resonances were finally fitted to model functions for the angular dependence (see SI, Figure S12):^[36]

$$I = A \left[P \cos^2 \theta \left(1 - \frac{3}{2} \sin^2 \beta \right) + \frac{1}{2} \sin^2 \beta \right] \quad (4)$$

with the specific amplitudes of the resonances (A), the degree of polarization ($P = 0.91$), the angle of incidence (θ), and the tilt angle of the transition dipole moment of the molecule with respect to the surface normal (β). The specified errors for the tilt angles come from the fit.

Synthesis and analytical data of target molecules 6, 7, 13, 14, and 18-21 (for all data cf. SI)

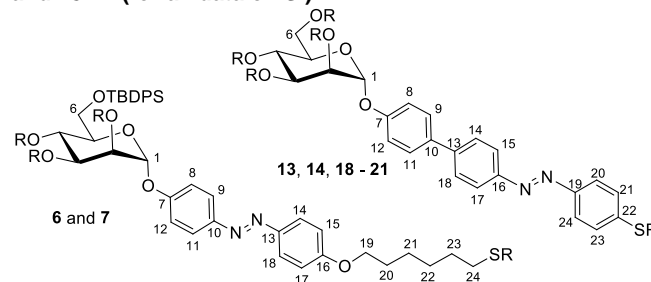


Figure 9. Compound numbering as used for the assignment of NMR spectroscopic data.

FULL PAPER for Chem. Eur. J.

(E)-p-[p'-(6-(Acetylthio)hexoxy)phenylazo]phenyl 2,3,4-tri-O-acetyl-6-O-tert-butylidiphenylsilyl- α -D-mannopyranoside (6):

The mannosyl donor **4** (337 mg, 905 μ mol) and the azobenzene derivative **5** (124 mg, 333 μ mol) were dissolved in dry dichloromethane (4 mL) and the solution was cooled to 0 °C and BF₃-etherate (0.17 mL, 1.36 mmol) added. The reaction mixture was warmed to room temperature and stirred for 2 h. Then, it was quenched by the addition of sat. aq. NaHCO₃ (4 mL), the phases were separated, and the organic phase was dried over MgSO₄, it was filtered and the filtrate was concentrated under reduced pressure. After column chromatography (toluene/ethyl acetate, 9:1) the product was obtained as an orange solid (258 mg, 287 μ mol, 86 %). R_f = 0.40 (toluene/ethyl acetate, 9:1); m.p. 139 °C; $[\alpha]^{20}_D +108.5$ (c = 0.73, ethyl acetate); ¹H-NMR (500 MHz, CDCl₃): δ = 7.89-7.81 (m, 4 H, H-9, H-11, H-14, H-18), 7.67-7.62 (m, 4 H, TBDPS-aryl-H_{ortho}), 7.44-7.34 (m, 6 H, TBDPS-aryl-H_{meta}, -H_{para}), 7.20-7.17 (m, 2 H, H-15, H-17), 7.00-6.97 (m, 2 H, H-8, H-12), 5.60 (d, ³J_{1,2} = 1.8 Hz, 1 H, H-1), 5.56 (m, 2 H, H-3, H-4), 5.45 (dd, ³J_{1,2} = 1.9 Hz, ³J_{2,3} = 3.2 Hz, 1 H, H-2), 4.03 (t, J = 6.5 Hz, 2 H, H-19), 3.92 (ddd, ³J_{4,5} = 9.3 Hz, ³J_{5,6a} = 4.5 Hz, ³J_{5,6b} = 1.9 Hz, 1 H, H-5), 3.76 (dd, ³J_{5,6a} = 4.6 Hz, ²J_{6a,6b} = 11.6 Hz, 2 H, H-6a), 3.67 (dd, ³J_{5,6b} = 2.0 Hz, ²J_{6a,6b} = 11.6 Hz, 2 H, H-6b), 2.90 (t, J = 7.3 Hz, 2 H, H-24), 2.33 (s, 3 H, SCOCCH₃), 2.18, 2.05, 1.92, (each s, each 3 H; 3 OAc), 1.85-1.79 (m, 2 H, H-20), 1.65-1.59 (dt, J = 14.7 Hz, J = 7.4 Hz, 2 H, H-23), 1.53-1.42 (m, 4 H, H-21, H-22), 1.03 (s, 9 H, C(CH₃)₃) ppm; ¹³C-NMR (126 MHz, CDCl₃): δ = 196.6 (SCOCCH₃), 170.2, 170.1, 169.5 (3 COCH₃), 161.4 (C-16), 157.5 (C-7), 148.3 (C-13), 146.9 (C-10), 135.8 (TBDPS-aryl-C_{ortho}), 135.6 (TBDPS-aryl-C_{ortho}), 133.3 (TBDPS-aryl-C_{ipso}), 133.0 (TBDPS-aryl-C_{ipso}), 129.7 (TBDPS-aryl-C_{para}), 129.7 (TBDPS-aryl-C_{para}), 127.7 (TBDPS-aryl-C_{meta}), 127.6 (TBDPS-aryl-C_{meta}), 124.5 (C-14, C-18), 124.2 (C-9, C-11), 116.7 (C-15, C-17), 114.7 (C-8, C-12), 95.7 (C-1), 72.0 (C-5), 69.6 (C-2), 69.2 (C-3), 68.1 (C-19), 65.9 (C-4), 62.3 (C-6), 30.7 (SCOCCH₃), 29.4 (C-23), 29.0 (C-19), 29.0 (C-20), 28.5 (C-22), 26.6 (C(CH₃)₃), 25.6 (C-21), 20.8, 20.8, 20.6 (3 COCH₃), 19.2 (C(CH₃)₃) ppm; IR (ATR): $\tilde{\nu}$ = 2932, 2857, 1752, 1213, 1106, 702, 502 cm⁻¹; MS (ESI): m/z : calcd. for C₄₈H₅₈N₂O₁₁SSi: 899.3603 [M]; found 899.3589.

(E)-p-[p'-(6-(Thio)hexoxy)phenylazo]phenyl-6-O-tert-butylidiphenylsilyl- α -D-mannopyranoside (7):

The protected mannoside **6** (250 mg, 278 μ mol) was dissolved in dry methanol (2 mL) and sodium methanolate solution (20 μ L, 5.4 M in methanol) was added. After stirring for 3 h at room temperature, the solution was neutralized with Amberlite IR120 ion exchange resin. The resin was filtered off and the crude was concentrated under reduced pressure. After filtration over silica, the product was obtained as an orange solid (200 mg, 273 μ mol, 90 %). $[\alpha]^{20}_D +20.0$ (c = 0.6, CH₂Cl₂); ¹H-NMR (500 MHz, CDCl₃): δ = 7.87-7.84 (m, 2 H, H-14, H-18), 7.82-7.78 (m, 2 H, H-9, H-11), 7.64-7.61 (m, 4 H, TBDPS-aryl-H_{ortho}), 7.43-7.30 (m, 6 H, TBDPS-aryl-H_{meta}, -H_{para}), 7.12-7.07 (m, 2 H, H-8, H-12), 6.99-6.96 (m, 2 H, H-15, H-17), 5.58 (d, ³J_{1,2} = 1.3 Hz, 1 H, H-1), 4.15 (s, 1 H, H-2), 4.08 (dd, ³J_{2,3} = 2.9 Hz, ³J_{3,4} = 9.3 Hz, 1 H, H-3), 4.04-3.96 (m, 3 H, H-4, H-19), 3.90 (d, ³J_{6,5} = 4.9 Hz, 2 H, H-6), 3.71 (ddd-dt, ³J_{5,6} = 5.0 Hz, ³J_{4,5} = 9.8 Hz, 1 H, H-5), 3.14 (s, 1 H, OH), 3.07 (s, 1 H, OH), 3.07 (s, 1 H, OH), 2.81 (s, 1 H, OH), 2.73-2.70 (m, 2 H, H-24), 1.86-1.81 (m, 2 H, H-20), 1.77-1.72 (m, 2 H, H-23), 1.68 (s, 1 H, SH), 1.54-1.48 (m, 4 H, H-21, H-22), 1.03 (s, 3 H, C(CH₃)₃) ppm; ¹³C-NMR (126 MHz, CDCl₃): δ = 161.3 (C-16), 157.7 (C-7), 148.2

(C-13), 146.9 (C-10), 135.6 (TBDPS-aryl-C_{ortho}), 135.5 (TBDPS-aryl-C_{ortho}), 132.7 (TBDPS-aryl-C_{ipso}), 132.7 (TBDPS-aryl-C_{ipso}), 130.0 (TBDPS-aryl-C_{para}), 127.8 (TBDPS-aryl-C_{meta}), 127.8 (TBDPS-aryl-C_{para}), 124.5 (C-14, C-18), 124.2 (C-9, C-11), 116.6 (C-15, C-17), 114.7 (C-8, C-12), 97.6 (C-1), 71.5 (C-5), 71.4 (C-3), 70.1 (C-2), 70.0 (C-4), 68.1 (C-19), 64.8 (C-6), 39.0 (C-24), 29.1 (C-20), 29.1 (C-23), 28.2 (C-22), 26.8 (C(CH₃)₃), 25.7 (C-21), 19.2 (C(CH₃)₃) ppm; MS (ESI): m/z : calcd. for C₄₀H₅₀N₂O₇SSi: 730.3125 [M]; found 730.3097; ϵ (ethyl acetate) = 19235 \pm 74.4 L x mol⁻¹ cm⁻¹.

(E)-p-[p'-(N,N-Dimethyl-S-thiocarbamoyl)phenylazo]biphenyl 2,3,4,6 tetra-O-acetyl- α -D-mannopyranoside (13):

The boronic ester **12** (100 mg, 243 μ mol), idoazobenzene **9**, potassium carbonate (102 mg, 738 μ mol) and TBABr were dissolved in water/toluene (1 : 2.5, 14 mL). The reaction mixture was degassed and after addition of a catalytic amount of tetrakis(triphenylphosphine)palladium(0), the reaction mixture was stirred at 80 °C for 4 h and then at room temperature overnight. The reaction mixture was diluted with ethyl acetate (30 mL) and brine (20 mL). The organic phase was dried over MgSO₄, it was filtered and the filtrate concentrated under reduced pressure. Column chromatography (cyclohexane/ethyl acetate, 2:1) gave the desired product as an orange solid (43.1 mg, 60.9 μ mol, 25 %). R_f = 0.27 (cyclohexane/ethyl acetate, 1:1); m.p. 182 °C; $[\alpha]^{20}_D +61.3$ (c = 0.91, CH₂Cl₂); ¹H-NMR (500 MHz, CDCl₃) δ = 8.0-7.98 (m, 2 H, H-14, H-18), 7.96-7.93 (m, 2 H, H-15, H-17), 7.71-7.69 (m, 2 H, H-20, H-24), 7.67-7.60 (m, 4 H, H-9, H-11, H-21, H-23), 7.21-7.18 (m, 2 H, H-8, H-12), 5.61-5.59 (m, 2 H, H-1, H-3), 5.49 (dd, ³J_{1,2} = 1.8 Hz, ³J_{2,3} = 3.5 Hz, 1 H, H-2), 5.40 (dd-t, ³J_{3,4} = ³J_{4,5} = 10.0 Hz, 1 H, H-4), 4.31 (dd, ³J_{5,6a} = 5.0 Hz, ²J_{6a,6b} = 12.0 Hz, 1 H, H-6a), 3.61 (dd, ³J_{5,6b} = 1.8 Hz, ²J_{6a,6b} = 10.9 Hz, 1 H, H-6b), 4.15-4.09 (m, 2 H, H-5, H-6b), 3.12, 3.06 (each s, each 3 H, 2 CH₃), 2.22, 2.07, 2.05, 2.05 (each s, each 3 H, 4 OAc) ppm; ¹³C-NMR (126 MHz, CDCl₃): δ = 170.5, 170.0, 170.0, 169.7 (4 COCH₃), 166.2 (SCO), 155.6 (C-7), 152.7 (C-10), 151.6 (C-13), 143.1 (C-16), 136.1 (C-21, C-23), 131.5 (C-19), 131.2 (C-22), 128.4 (C-9, C-11), 127.4 (C-20, C-24), 123.6 (C-14, C-18), 123.1 (C-15, C-17), 116.9 (C-8, C-12), 95.8 (C-1), 69.4 (C-2), 69.3 (C-5), 68.9 (C-3), 65.9 (C-4), 62.1 (C-6), 37.0 (CH₃), 20.9, 20.7, 20.7 20.7 (4 COCH₃) ppm; IR (ATR): $\tilde{\nu}$ = 2937, 1745, 1214, 1034, 826 cm⁻¹; MS (ESI): m/z : calcd for C₃₅H₃₇O₁₁N₃S + Na⁺: 703.2041 [M]; found 730.2026; EA: calcd. for C₃₅H₃₇O₁₁N₃S: C, 59.40; H, 5.27; N, 5.94; S, 4.53 %, found: C, 58.57; H, 4.903; N, 6.21; S, 4.75 %.

(E)-p-[p'-Mercaptophenylazo]biphenyl- α -D-mannopyranoside (14):

The thiocarbamate **13** (16.7 mg, 23.5 μ mol) suspended in methanol (1 mL) and potassium hydroxide solution (0.2 mL, 4.3 M, in MeOH) was added. The reaction solution was stirred for 1 h. Then, the same amount of potassium hydroxide solution (0.2 mL, 4.3 M, in MeOH) was added and the reaction solution was stirred for 16 h at room temperature. It was neutralized with 2 M HCl and concentrated under reduced pressure. Potassium chloride was precipitated by addition of acetone and filtered off. The solvent was removed under reduced pressure and the product was obtained as an orange solid (7.3 mg, 68 %). $[\alpha]^{20}_D +29.3$ (c = 0.02, MeOH); ¹H-NMR (500 MHz, DMSO-*d*₆) δ = 7.88-7.94 (m, 4 H, H-15, H-17, H-20, H-24), 7.88-7.87 (m, 2 H, H-15, H-17), 7.81-7.79 (m, 2 H, H-21, H-23), 7.74-7.72 (m, 2 H, H-9, H-11), 7.22-7.12 (m, 2 H, H-8, H-12), 5.47 (d,

FULL PAPER for Chem. Eur. J.

$^3J_{1,2} = 1.3\text{ Hz}$, 1 H, H-1), 3.87 (m, 1 H, H-3), 3.71 (m, 1 H, H-2) ppm. $^{13}\text{C-NMR}$ (126 MHz, DMSO- d_6): $\delta = 156.5$ (C-10), 151.1 (C-22), 150.5 (C-13), 142.7 (C-16), 138.9 (C-19), 132.3 (C-7), 127.9 (C-9, C-11), 127.6 (C-21, C-23), 127.0 (C-14, C-18), 123.5 (C-20, C-24), 123.2 (C-15, C-17), 117.1 (C-8, C-12), 98.6 (C-1), 74.9 (C-5), 70.5 (C-3), 69.9 (C-2), 66.5 (C-4), 60.0 (C-6) ppm; IR (ATR): $\tilde{\nu} = 1589, 1131, 1001, 825, 557\text{ cm}^{-1}$; MS (ESI): m/z : calcd. for $\text{C}_{24}\text{H}_{34}\text{O}_6\text{N}_2\text{S} + \text{H}^+$: 469.1428 [M]; found 469.1423, ϵ (DMSO) = $3756.39 \pm 36.0\text{ L} \times \text{mol}^{-1}\text{ cm}^{-1}$.

(E)-p-[p'-(N,N-Dimethyl-S-thiocarbamoyl)biphenylazo]phenyl 2,3,4,6 tetra-O-acetyl- α -D-mannopyranoside (18): The boronic ester **17** (23.6 mg, 36.1 μmol), the thiocarbamate **15** (10.0 mg, 30.5 μmol), potassium carbonate (4.8 mg, 61.0 μmol) and TBABr (5.0 mg, 15.5 μmol) were dissolved in a toluene/H₂O mixture (2:1, 6 ml) and degassed and after addition of a catalytic amount of tetrakis(triphenylphosphine)palladium(0), the reaction mixture was stirred at 80 °C for 4 h and 16 h at room temperature. The phases were separated, the organic phase was washed with water (10 mL) and dried over MgSO₄. It was filtered and the solvent removed under reduced pressure and purified by column chromatography (cyclohexane/ethyl acetate, 1:1). The product was obtained as an orange solid (10.3 mg, 14.6 μmol , 48 %). $R_f = 0.35$ (cyclohexane/ethyl acetate, 1:1); m.p. 182 °C; $[\alpha]^{20\text{D}} +85.6$ ($c = 0.15$, CH₂Cl₂); $^1\text{H-NMR}$ (500 MHz, CDCl₃) $\delta = 7.99$ -7.92 (m, 4 H, H-9, H-11, H-14, H-18), 7.75-7.51 (m, 6 H, H-15, H-17, H-20, H-21, H-23, H-24), 7.26-7.20 (m, 2 H, H-8, H-12), 5.61 (m, 2 H, H-1, H-3), 5.49 (dd, $^3J_{1,2} = 1.8\text{ Hz}$, $^3J_{2,3} = 3.4\text{ Hz}$, 1 H, H-2), 5.40 (dd-t, $^3J_{3,4} = ^3J_{4,5} = 9.8\text{ Hz}$, 1 H, H-4), 4.33 (m, 1 H, H-6a), 4.15-4.05 (m, 2 H, H-5, H-6b), 3.09 (s, 6 H, 2 CH₃), 2.22, 2.06, 2.05, 2.04 (each s, each 3 H, 4 OAc) ppm; $^{13}\text{C-NMR}$ (126 MHz, CDCl₃): $\delta = 170.5, 170.0, 170.0, 196.7$ (4 COCH₃), 166.8 (SCO), 157.6 (C-7), 151.9 (C-13), 148.5 (C-10), 142.7 (C-16), 141.1 (C-19), 136.3 (C-22), 136.1 (C-21, 23), 127.9 (C-15, C-17), 127.7 (C-20, C-24), 123.9 (C-14, C-18), 95.7 (C-1), 69.4 (C-5), 69.3 (C-2), 68.8 (C-3), 65.9 (C-4), 62.1 (C-6), 37.0 (2 CH₃), 20.9, 20.7, 20.7 (4 COCH₃) ppm; IR (ATR): $\tilde{\nu} = 1746, 1365, 1211, 1030, 819\text{ cm}^{-1}$; MS (ESI): m/z : calcd. for $\text{C}_{35}\text{H}_{38}\text{O}_{11}\text{N}_3\text{S}$: 708.2222 [M]; found 708.2223.

(E)-p-[p'-(N,N-Dimethyl-S-thiocarbamoyl)biphenylazo]phenyl 2,3,4,6 tetra-O-allyl- α -D-mannopyranoside (19): The boronic ester **17** (241 mg, 373 μmol), the thiocarbamate **15** (247 mg, 804 μmol), cesium carbonate (237 mg, 727 μmol) and TBABr (25 mg, 78 μmol) were dissolved in toluene/H₂O (10:1, 6 mL). The solution was degassed and tetrakis(triphenylphosphine)palladium was added (57 mg, 49 μmol). The reaction mixture was stirred at 90 °C for 16 h, diluted with ethyl acetate (30 mL) and washed with 2 M aq. HCl (20 mL). The organic phase was dried over MgSO₄, filtered, and the filtrate concentrated under reduced pressure. Column chromatography (cyclohexane / ethyl acetate, 4:1) gave the product as an orange oil (70 mg, 100 μmol , 27 %). $R_f = 0.05$ (cyclohexane/ethyl acetate, 2:1); $[\alpha]^{20\text{D}} +95.0$ ($c = 0.10$, CH₂Cl₂); $^1\text{H-NMR}$ (600 MHz, CDCl₃) $\delta = 7.97$ -7.90 (m, 4 H, H-9, H-11, H-14, H-18), 7.74-7.72 (m, 2 H, H-16, H-17), 7.68-7.66 (m, 2 H, H-20, H-24), 7.60-7.58 (m, 2 H, H-21, H-23), 7.21-7.19 (m, 2 H, H-8, H-12), 6.04-5.85 (m, 4 H, HC=CH₂), 5.65 (d, $^3J_{1,2} = 1.5\text{ Hz}$, 1 H, H-1), 5.40-5.22 (m, 6 H, 3 HC=CH₂), 5.16-5.12 (m, 2 H, HC=CH₂), 4.38 (ddt, $^4J_{\text{OCH}_2, \text{CH}=\text{CH}_2} = 1.3\text{ Hz}$, $^3J_{\text{OCH}_2, \text{CH}=\text{CH}_2} = 5.7\text{ Hz}$, $^2J_{\text{OCH}_a, \text{OCH}_b} = 12.3\text{ Hz}$, 1 H, OCH), 4.29-4.21 (m, 4 H, 2 OCH₂), 4.13 (m, 1 H,

OCH), 4.08 (m, 1 H, OCH), 3.97-3.87 (m, 4 H, H-2, H-3, H-4, OCH), 3.73 (m, 1 H, H-5), 3.69 (dd, $^3J_{5,6a} = 4.3\text{ Hz}$, $^2J_{6a,6b} = 10.9\text{ Hz}$, 1 H, H-6a), 3.61 (dd, $^3J_{5,6b} = 1.8\text{ Hz}$, $^2J_{6a,6b} = 10.9\text{ Hz}$, 1 H, H-6b), 3.13, 3.06 (each s, each 3 H, CH₃) ppm; $^{13}\text{C-NMR}$ (150 MHz, CDCl₃): $\delta = 166.8$ (SCO), 158.5 (C-7), 152.0 (C-13), 148.0 (C-10), 142.5 (C-22), 141.1 (C-16), 136.3 (C-19), 135.0, 134.9, 134.8, 134.7 (HC=CH₂), 127.9 (C-15, C-17), 127.6 (C-21, C-32), 124.6 (C-14, C-18), 123.3 (C-9, C-11), 117.8 (OCH₂CH=CH₂), 116.9 (OCH₂CH=CH₂), 116.8 (OCH₂CH=CH₂), 116.7 (C-8, C-12), 116.6 (OCH₂CH=CH₂), 96.5 (C-1), 79.1 (C-2), 74.5 (C-3), 74.4 (C-4), 74.0 (OCH₂CH=CH₂), 72.4 (C-5), 72.4 (OCH₂CH=CH₂), 72.3 (OCH₂CH=CH₂), 71.4 (OCH₂CH=CH₂), 68.7 (C-6), 37.0 (2 CH₃) ppm; IR (ATR): $\tilde{\nu} = 2920, 2853, 1668, 1233, 1130, 1088, 987\text{ cm}^{-1}$; MS (ESI): m/z : calcd. for $\text{C}_{39}\text{H}_{45}\text{O}_7\text{N}_3\text{S} + \text{Na}^+$: 722.2870 [M]; found 722.2857.

(E)-p-[p'-Mercaptobiphenylazo]phenyl α -D-mannopyranoside (20): The carbamate **18** (37 mg, 55 μmol) and potassium hydroxide (115 mg, 2.03 mmol) was dissolved in methanol, degassed with ultrasound for 10 minutes and was stirred for 2 h at 80 °C. The reaction mixture was neutralized with 2 N HCl and concentrated under reduced pressure. The residue was dissolved in acetone and filtered to remove precipitated potassium chloride. After removal of the solvent, the product was obtained as an orange amorphous solid (16.5 mg, 35 μmol). $[\alpha]^{20\text{D}} +66.7$ ($c = 0.09$, DMSO); $^1\text{H-NMR}$ (500 MHz, DMSO- d_6) $\delta = 7.91$ -7.87 (m, 6 H, H-9, H-11, H-14, H-18, H-15, H-17), 7.85-7.81 (m, 2 H, H-20, H-24), 7.71-7.69 (m, 2 H, H-21, H-23), 7.29-7.27 (m, 2 H, H-8, H-12), 5.55 (d, $^3J_{1,2} = 1.4\text{ Hz}$, 1 H, H-1), 5.10 (m, 1 H, OH), 4.86 (m, 1 H, OH), 4.80 (m, 1 H, OH), 4.46 (m, 1 H, OH), 3.87 (m, 1 H, H-3), 3.70 (m, H-2), 3.60 (m, 1 H, H-6a), 3.52-3.50 (m, 2 H, H-4, H-6b) ppm; $^{13}\text{C-NMR}$ (500 MHz, DMSO- d_6) $\delta = 158.9$ (C-13), 151.2 (C-10), 146.8 (C-7), 141.2 (C-16), 138.2 (C-22), 135.5 (C-19), 127.8 (C-20, C-24), 127.7 (C-21, C-23), 127.4 (C-15, C-17), 124.3 (C-9, C-11), 122.9 (C-14, C-18), 117.02 (C-8, C-12), 98.5 (C-1), 75.2 (C-5), 70.4 (C-3), 69.7 (C-2), 66.6 (C-4), 60.9 (C-6) ppm; IR (ATR): $\tilde{\nu} = 3249, 2923, 1589, 1131, 1006, 2848, 557\text{ cm}^{-1}$; MS (ESI): m/z : calcd. for $\text{C}_{24}\text{H}_{24}\text{O}_6\text{N}_2\text{S}$: 468.1355 [M]; found 468.1353; ϵ (DMSO) = $17631.11 \pm 302.48\text{ L} \times \text{mol}^{-1}\text{ cm}^{-1}$.

(E)-p-[p'-Mercaptobiphenylazo]phenyl 2,3,4,6 tetra-O-allyl- α -D-mannopyranoside (21): The carbamate **19** (26.2 mg, 37.4 μmol) and potassium hydroxide (106 mg, 188 mmol) were dissolved in methanol (2 mL) and the reaction mixture degassed with ultrasound for 10 minutes. The reaction mixture was stirred at 65 °C for one h and then 16 h at room temperature. It was neutralized with ion exchange resin Amberlite IR120, the resin was filtered off, and the filtrate was concentrated under reduced pressure. The product was obtained as a dark orange syrup (11.6 mg, 18.4 μmol , 48 %). $[\alpha]^{20\text{D}} +97.1$ ($c = 0.07$, CH₂Cl₂); $^1\text{H-NMR}$ (600 MHz, CDCl₃) $\delta = 7.97$ -7.91 (m, 4 H, H-9, H-11, H-14, H-18), 7.74-7.72 (m, 2 H, H-16, H-17), 7.68-7.66 (m, 2 H, H-20, H-24), 7.60-7.58 (m, 2 H, H-21, H-23), 7.21-7.19 (m, 2 H, H-8, H-12), 6.04-5.85 (m, 4 H, HC=CH₂), 5.65 (d, $^3J_{1,2} = 1.5\text{ Hz}$, 1 H, H-1), 5.40-5.22 (m, 6 H, 3 HC=CH₂), 5.16-5.12 (m, 2 H, HC=CH₂), 4.38 (ddt, $^4J_{\text{OCH}_2, \text{CH}=\text{CH}_2} = 1.3\text{ Hz}$, $^3J_{\text{OCH}_2, \text{CH}=\text{CH}_2} = 5.7\text{ Hz}$, $^2J_{\text{OCH}_a, \text{OCH}_b} = 12.3\text{ Hz}$, 1 H, OCH), 4.29-4.21 (m, 4 H, 2 OCH₂), 4.13 (m, 1 H, OCH), 4.08 (m, 1 H, OCH), 3.97-3.87 (m, 4 H, H-2, H-3, H-4, OCH), 3.73 (m, 1 H, H-5), 3.69 (dd, $^3J_{5,6a} = 4.3\text{ Hz}$, $^2J_{6a,6b} = 10.9\text{ Hz}$, 1 H, H-6a), 3.61 (dd, $^3J_{5,6b} = 1.8\text{ Hz}$, $^2J_{6a,6b} = 10.9\text{ Hz}$, 1 H, H-

FULL PAPER for Chem. Eur. J.

6b), 3.52 (s, 1 H, SH) ppm; ^{13}C -NMR (150 MHz, CDCl_3): δ = 158.6 (C-7), 152.0 (C-13), 148.0 (C-10), 135.0, 135.0, 134.9, 134.7 (HC=CH₂), 131.0 (C-23), 129.8 (C-21), 128.2 (C-24), 127.8 (C-20), 127.8 (C-16), 127.7 (C-19), 127.6 (C-15, C-17), 127.4 (C-22), 124.7 (C-14, C-18), 123.3 (C-9, C-11), 117.8 (OCH₂CH=CH₂), 116.9 (OCH₂CH=CH₂), 116.8 (OCH₂CH=CH₂), 116.7 (C-8, C-12), 116.6 (OCH₂CH=CH₂), 96.5 (C-1), 79.2 (C-2), 74.5 (C-3), 74.4 (C-4), 74.0 (OCH₂CH=CH₂), 72.4 (C-5), 72.4 (OCH₂CH=CH₂), 72.3 (OCH₂CH=CH₂), 71.4 (OCH₂CH=CH₂), 68.7 (C-6) ppm; IR (ATR): $\tilde{\nu}$ = 2921, 2856, 1597, 1497, 1233, 1130, 1102, 986 cm^{-1} ; MS (ESI): m/z calcd. for $\text{C}_{36}\text{H}_{40}\text{O}_6\text{N}_2\text{S} + \text{Na}^+$: 722.2870 [M]; found 722.2857; ϵ (CHCl_3) = 26549.98 \pm 298.19 L \times mol⁻¹ cm⁻¹.

Acknowledgements

We thank the Deutsche Forschungsgemeinschaft for financial support of projects B11, C01 and C11 within SFB 677. Furthermore, we would like to thank the Helmholtz-Zentrum Berlin for providing the beamtime at the HE-SGM beamline (XPS & NEXAFS Measurements) and Prof. Christof Wöll (KIT) for providing the Prevac endstation with support by Dr. Alexei Nefedov (also KIT).

Keywords: Glyco-SAMs • Azobenzenes • Photochemistry • IRRAS • Photoswitchable Carbohydrate Orientation

- [1] A. Varki, R. D. Cummings, J. D. Esko, P. Stanley, G. W. Hart, M. Aebi, A. G. Darvill, T. Kinoshita, N. H. Packer, J. H. Prestegard, R. L. Schnaar, P. H. Seeberger, Eds, *Essentials of glycobiology*; Cold Spring Harbor Laboratory Press, New York, **2017**.
- [2] M. Ambrosi, N. R. Cameron, B. G. Davis, *Org. Biomol. Chem.* **2005**, *3*, 1593–1608.
- [3] P. Chahales, D. G. Thanassi, *Microbiol. Spec.* **2015**, *3(5)*:10.1128/microbiolspec.UTI-0018-2013.
- [4] J. Poole, C. J. Day, M. v. Itzstein, J. C. Paton, M. P. Jennings, *Nature Rev. Microbiol.* **2018**, *16(7)*, 440–452.
- [5] a) N. Laurent, J. Voglmeir, S. L. Flitsch, *Chem. Comm.* **2008**, *37*, 4400–4412; b) L. Ban, M. Mrksich, *Angew. Chem. Int. Ed.* **2008**, *47*, 3396–3399; c) Y. Liu, A. S. Palma, T. Feizi, *Biol. Chem.* **2009**, *390*, 647–656; d) P. M. Dietrich, T. Horlacher, P.-L. Girard-Laurialt, T. Gross, A. Lippitz, H. Min, T. Wirth, R. Castelli, P. H. Seeberger, W. E. S. Unger, *Langmuir* **2011**, *27*, 4808–4815; e) C. Grabosch, M. Kind, Y. Gies, F. Schweighöfer, A. Terfort, T. K. Lindhorst, *Org. Biomol. Chem.* **2013**, *11*, 4006–4015; f) J. K. Bhattarai, D. Neupane, V. Mikhaylov, A. V. Demchenko, K. J. Stine in *Carbohydrate*; (Eds. M. Caliskan, I. H. Kavakli, G. C. Oz), IntechOpen **2017**, 63; g) Z.-L. Zhi, N. Laurent, A. K. Powell, R. Karamanska, M. Fais, J. Voglmeir, A. Wright, J. M. Blackburn, P. R. Crocker, D. A. Russell, S. Flitsch, R. A. Field, J. E. Turnbull, *ChemBioChem* **2008**, *9*, 1568–1575; h) I. Tavernaro, S. Hartmann, L. Sommer, H. Hausmann, C. Rohner, M. Ruehl, A. Hoffmann-Roeder, S. Schlecht, *Org. Biomol. Chem.* **2015**, *13*, 81–97.
- [6] V. Chandrasekaran, H. Jacob, F. Petersen, K. Kathirvel, F. Tuzcek, T. K. Lindhorst, *Chem. Eur. J.* **2014**, *20*, 8744–8752.
- [7] T. Weber, V. Chandrasekaran, I. Stamer, M. B. Thygesen, A. Terfort, T. K. Lindhorst, *Angew. Chem. Int. Ed.* **2014**, *53*, 14583–14586.
- [8] a) L. Möckl, A. Müller, C. Bräuchle, T. K. Lindhorst, *Chem. Comm.* **2016**, *52*, 1254–1257; b) G. Despras, L. Möckl, A. Heitmann, I. Stamer, C. Bräuchle, T. Lindhorst, *ChemBioChem* **2019**, *20*, 2373–2382.
- [9] J. C. Love, L. A. Estroff, J. K. Kriebel, R. G. Nuzzo, G. M. Whitesides, *Chem. Rev.* **2005**, *105*, 1103–1169.
- [10] R. Klajn, *Pure Appl. Chem.* **2010**, *82*, 2247–2279.
- [11] W. R. Browne, B. L. Feringa, *Annu. Rev. Phys. Chem.* **2009**, *60*, 407–428.
- [12] J. Zhang, J. K. Whitesell, M. A. Fox, *Chem. Mater.* **2001**, *13*, 2323–2331.
- [13] a) B. Baisch, D. Raffa, U. Jung, O. M. Magnussen, C. Nicolas, J. Lacour, J. Kubitschke, R. Herges, *J. Am. Chem. Soc.* **2009**, *131*, 442–443; b) U. Jung, C. Schütt, O. Filinova, J. Kubitschke, R. Herges, O. Magnussen, *J. Phys. Chem. C* **2012**, *116*, 25943–25948; c) A. Schlimm, R. Löw, T. Rusch, F. Röhrich, T. Strunskus, T. Tellkamp, F. Sönnichsen, U. Manthe, O. Magnussen, F. Tuzcek, R. Herges, *Angew. Chem. Int. Ed.* **2019**, *58*, 6574–6578.
- [14] H. Jacob, S. Ulrich, U. Jung, S. Lemke, T. Rusch, C. Schütt, F. Petersen, T. Strunskus, O. Magnussen, R. Herges, F. Tuzcek, *Phys. Chem. Chem. Phys.* **2014**, *16*, 22643–22650.
- [15] J. Lahann, S. Mitragotri, T.-N. Tran, H. Kaido, J. Sundaram, I. S. Choi, S. Hoffer, G. A. Somorjai, R. Langer, *Science* **2003**, *299*, 371–374.
- [16] G. Pace, V. Ferri, C. Grave, M. Elbing, C. von Hänisch, M. Zhamnikov, M. Mayor, M. A. Rampi, P. Samori, *Proc. Natl. Acad. Sci. USA* **2007**, *104*, 9937–9942.
- [17] J. Zhang, P. Kovac, *J. Carbohydr. Chem.* **1999**, *18*, 461–469.
- [18] J. K. Fairweather, T. Karoli, V. Ferro, *Bioorg. Med. Chem.* **2004**, *12*, 6063–6075.
- [19] V. Chandrasekaran, E. Johannes, H. Kobarg, F. D. Sönnichsen, T. K. Lindhorst, *ChemistryOpen* **2014**, *3*, 99–108.
- [20] N. Miyaura, A. Suzuki, *Chem. Rev.* **1995**, *95*, 2457–2483.
- [21] Z. Han, J. S. Pinkner, B. Ford, E. Chorell, J. M. Crowley, C. K. Cusumano, S. Campbell, J. P. Henderson, S. J. Hultgren, J. W. Janetka, *J. Med. Chem.* **2012**, *55*, 3945–3959.
- [22] A. Perjessy, R. G. Jones, S. L. McClair, J. M. Wilkins, *J. Org. Chem.* **1983**, *48*, 1266–1271.
- [23] J. M. Chalker, C. S. C. Wood, B. G. Davis, *J. Am. Chem. Soc.* **2009**, *131*, 16346–16347.
- [24] C. Kallweit, G. Haberhauer, S. Woitschetzki, *Chem. Eur. J.* **2014**, *20*, 6358–6365.
- [25] a) J. Strueben, M. Lipfert, J.-O. Springer, C. A. Gould, P. J. Gates, F. D. Sönnichsen, A. Staubitz, *Chem. Eur. J.* **2015**, *21*, 11165–11173; b) A. Moanta, *J. Chil. Chem. Soc.* **2014**, *59*, 2275–2278.
- [26] U. Jung, S. Kuhn, U. Cornelissen, F. Tuzcek, T. Strunskus, V. Zaporotchenko, J. Kubitschke, R. Herges, O. Magnussen, *Langmuir* **2011**, *27*, 5899–5908.
- [27] S. Ulrich, U. Jung, T. Strunskus, C. Schütt, A. Bloedorn, S. Lemke, E. Ludwig, L. Kipp, F. Faupel, O. Magnussen, R. Herges, *Phys. Chem. Chem. Phys.* **2015**, *17*, 17053–17062.
- [28] H. Jacob, K. Kathirvel, F. Petersen, T. Strunskus, A. Bannwarth, S. Meyer, F. Tuzcek, *Langmuir* **2013**, *29*, 8534–8543.
- [29] L. Hallmann, A. Bashir, T. Strunskus, R. Adelung, V. Staemmler, C. Wöll, F. Tuzcek, *Langmuir* **2008**, *24*, 5726–5733.
- [30] H. Wackerbarth, R. Marie, M. Grubb, J. Zhang, A. G. Hansen, I. Chorkendorff, C. B. V. Christensen, A. Boisen, J. Ulstrup, *J. Solid State Electr.* **2004**, *8*, 474–481.
- [31] a) R. G. Nuzzo, F. A. Fusco, D. L. Allara, *J. Am. Chem. Soc.* **1987**, *109*, 2358–2368; b) Z. Hou, S. Dante, N. L. Abbott, P. Stroeve, *Langmuir* **1999**, *15*, 3011–3014; c) M. D. Porter, T. B. Bright, D. L. Allara, C. E. D. Chidsey, *J. Am. Chem. Soc.* **1987**, *109*, 3559–3568; d) L. H. Dubois, R. G. Nuzzo, *Annu. Rev. Phys. Chem.* **1992**, *43*, 437–463.
- [32] R. G. Greenler, *J. Chem. Phys.* **1966**, *44*, 310–315.
- [33] a) A. Cembran, F. Bernardi, M. Garavelli, L. Gagliardi, G. Orlandi, *J. Am. Chem. Soc.* **2004**, *126*, 3234–3243; b) A. R. A. Mostard, *Acta Chem. Scand.* **1971**, *25*, 3561–3568.
- [34] a) A. Turchanin, D. Käfer, M. El-Desawy, C. Wöll, G. Witte, A. Gölzhäuser, *Langmuir* **2009**, *25*, 7342–7352; b) W. Geyer, V. Stadler, W. Eck, M. Zhamnikov, A. Gölzhäuser, M. Grunze, *Appl. Phys. Lett.* **1999**, *75*, 2401–2403; c) S. Frey, H.-T. Rong, K. Heister, Y.-J. Yang, M. Buck, M. Zhamnikov, *Langmuir* **2002**, *18*, 3142–3150; d) A. Shaporenko, K. Rössler, H. Lang, M. Zhamnikov, *J. Phys. Chem. B* **2006**, *110*, 24621–24628; e) W. Azzam, B. I. Wehner, R. A. Fischer, A. Terfort, C. Wöll, *Langmuir* **2002**, *18*, 7766–7769; f) P. Cyganik, M. Buck, T. Strunskus, A.

FULL PAPER for Chem. Eur. J.

Shaporenko, J. Wilton Ely, M. Zharnikov, C. Wöll, *J. Am. Chem. Soc.* **2004**, *126*, 5960–5961. [36] J. Stöhr, D. A. Outka, *Phys. Rev. B* **1987**, *36*, 7891–7905.

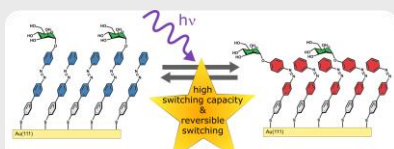
[35] A. E. McDermott, T. Polenova, *Solid State NMR Studies of Biopolymers*; Wiley, **2012**.

WILEY-VCH

Accepted Manuscript

Entry for the Table of Contents

FULL PAPER



Ellen Fast^{[a]#}, Alexander Schlimm^{[b]#},
Irene Lautenschläger^[b], Kai Uwe
Clausen^[b], Thomas Strunskus^[c], Carina
Spormann^[e], Thisbe K. Lindhorst^{[a]*},
Felix Tuczek^{[b]*}

Page No. – Page No.

Improving the Switching Capacity of
Glyco-SAMs on Au(111)

Glyco-SAMs were fabricated on Au(111) and their photoswitching properties were extensively investigated with a powerful set of methods (IRRAS, XPS and NEXAFS). In order to maximize the photoswitching capacity different concepts for the assembly of the underlying SAM were evaluated.